MPS/Int. LIN/68-3
21 May, 1968

PROPOSAL FOR THE LAYOUT OF THE BEAM TRANSPORT SYSTEM LINAC-SYNCHROTRON INJECTOR

M. Weiss

PS/6565

Summary

This report studies the problem of transporting the linac beam and injecting it into the new synchrotron injector, SI, for the PS.

The problem is defined in the introduction, followed by a section dealing with the choice of a vertical deflection system which bends the linac beam successively into the four vertically stacked SI rings.

In the next section are established the conditions in the transverse phase planes which are imposed on the beam transport design. The beam matching computations are based on these conditions.

The longitudinal phase plane is treated in section 5. For absolute energy and energy spread measurements a design of a separate measuring line is proposed in section 7. The beam is deflected into this line between beam pulses injected into the SI.

The proposed layout of the beam transport system is described in section 8. and presented on a drawing.

The report concludes with an appendix dealing with analytical space charge calculations. As in other similar treatments, simplifications are made. However, they are chosen in such a way as to overestimate the space charge influence on the beam transport.

Symbols

The elements in the new part of the beam transport system linac-SI (henceforth called injection line) are indicated by two or three letters, followed, if necessary, by one or two numbers. The first letter is I (injection) or M (measuring line); the second and third letters describe the kind of the element, The first number refers to the position in the line, the second one corresponds to the number of the SI ring.

IB, MB	bending magnet (horizontal bend)
IQ, MQ	quadrupole
IEV	vertical electrostatic deflector
IEH	horizontal electrostatic deflector
IBV	vertical bending magnet
ID	horizontal deflection magnet for injection
IDB	debuncher
IDE	emittance display device
MFC	Faraday cup
IA, MA	4 jaw apertures
IS, MS	steering coil
IPU	pick-up electrodes
ITV	TV screen and camera

The emittance and acceptance ellipses in the transverse phase planes are denoted as follows:

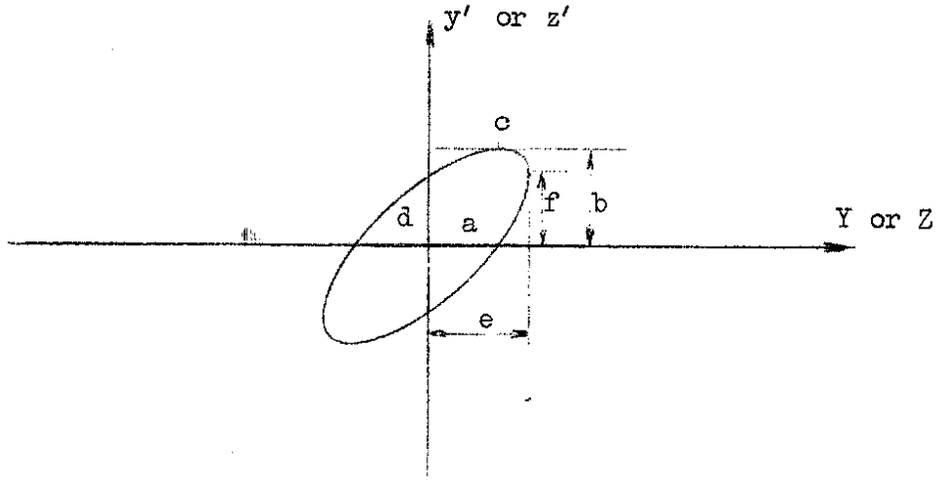

Index

1. INTRODUCTION

Definition of the injection line.

The injection line for the SI has to ensure the transport and injection of the linac beam into this machine. At the same time, the possibility of injecting directly into the PS should be maintained with a beam switching capacity such as to allow an alternate operation between SI and PS. For the full use of both these machines (max. repetition rate = 1 p/s), the linac has to pulse twice a second and the switching has to be done in less than 0.5 s.

A special feature of the injection line is the vertical deflection system necessary to inject the beam into the four vertically stacked SI rings.

Fig. 1 shows a scheme of the injection line. The part to the left of the bending magnet IB1 exists, the proposal for the layout of the remainder ($\sim$ 77 m) is the purpose of this paper.

Requirements.

The basic considerations concerning the injection line are described in The Second Stage CPS Improvement Study, MPS/Int. DL/B 67-19. For the sake of completeness we group here some important topics on which the design of the line is based :

1) Linac beam characteristics :

- current ..... 100 mA
- emittance (unnormalised) in each of the transverse phase planes ..... $30\pi.10^{-6}$ rad m

  (The characteristics of the actual linac beam are shown in Fig. 2).
- energy spread (after debunching) ..... $\leq$ 150 keV
- beam pulse length ('good beam') ..... $\sim$ 80 μs

2) Matching :

- the beam emittance has to be matched to the SI acceptance in both transverse phase planes. The matching in the horizontal phase plane depends on the number of injected turns.

- in the horizontal phase plane the beam has to be achromatic*. The injection line should therefore, if possible, be without horizontal bends (with the exception of the bend at the injection point).
- in the vertical phase plane, due to deflection and energy spread in the beam, the emittance will increase somewhat. An increase of a few percent can be tolerated because the vertical SI acceptance is ~ 30% bigger than the linac emittance . A certain blow-up of the vertical emittance is also expected later in the SI due to the action of space charge in a dense beam with elliptical cross-section.

Space charge action.

The linac beam, during its transport to the SI, is subjected to space charge action which tends to dilute its dense core. The space charge action is especially strong just after the linac, where the beam bunches have the minimum azimuthal length and the particle density is maximum. Some measurements made in the linac Group predict, however, that the dilution over the ~ 95 m of beam transport from linac to SI will not be considerable.

An estimate of space charge action is presented in Appendix 1 in order to see to what extent this can increase the required strength of lenses or ask for a larger cross-section of the injection vacuum chamber. It was found that the beam cross-section in the injection line is such as to make corrections for space charge action negligible.

2. CHOICE OF THE VERTICAL DEFLECTION SYSTEM

Before considering the design of the injection line, a choice has to be made concerning the vertical deflection system. As a consequence of this choice several conditions will be imposed on the layout of the injection line.

---

* It can be shown that for the kind of multiturn injection that is planned for SI (where an appreciable portion of the beam is scraped off at each injected turn), an achromatic injection is superior ro an injection with α_p, α_p' matching. With an achromatic injection one scrapes off more particles with an energy error, but beam centers of different injected turns are closer together, resulting ultimately in a denser SI beam.

The main requirements put on a vertical deflection system are the following :

- injection into the four SI rings, displaced 350 mm from each other
- injection into each ring continously variable from 0 to 20 μs,
- rapid change-over from one ring to the next, of the order of 100 ns (to reduce radioactivity induced by beam losses).

Comparison between electrostatic and magnetic devices

In principle the vertical deflection can be produced either by kicker magnets or by an electrostatic deflector.

To compare these two devices, we put down some expressions :

Magnetic force : $Fm = qv_pB$ $\quad v_p$ .... particle velocity

Electric force : $Fe = qE$

For equal deflection :

$$v_pB = E \quad \text{or} \quad \beta c\, B = E \qquad c \text{ .... velocity of light}$$

The ratio of stored energies (both devices have equal length and aperture) is :

$$\frac{We}{Wm} = \frac{\frac{\epsilon_0 E^2}{2}}{\frac{B^2}{2\mu_0}} = \frac{\epsilon_0 \mu_0 E^2}{B^2} = \left(\frac{v_p}{c}\right)^2 = \beta^2$$

One has to take into account that in the case of a magnetic kicker, the energy flows the whole time the deflection is needed. Therefore the ratio between electric and magnetic energy necessary for a given deflection is :

$$\frac{We}{Wm} = \frac{\beta^2}{t/\tau} = \beta^2 \frac{\tau}{t}$$

where t is the deflection time and τ the kicker rise time.

Example : $t = 2\ \mu s$

$\tau = 100$ ns

$\beta = 0.314$ (at 50 MeV)

$$\frac{We}{Wm} \simeq 10^{-1} \frac{10^{-7}}{2.10^{-6}} = \frac{1}{200} \quad \text{or} \quad Wm = 200\ We$$

For longer deflection time t, the energy ratio becomes still more favourable for an electrostatic device.

The consequences of smaller energy in an electrostatic device are simpler spark gaps (or thyratrons), matching resistors and power supplies. In addition, other advantages of an electrostatic device are :

- mechanical simplicity,
- no pulse forming network is needed,
- variable deflection time is easily obtained.

An electrostatic deflector will have several pairs of electrodes. To switch over the injection from one ring to another, a pair of electrodes will be discharged. How long is this discharge time ?

The discharge circuit is presented schematically :

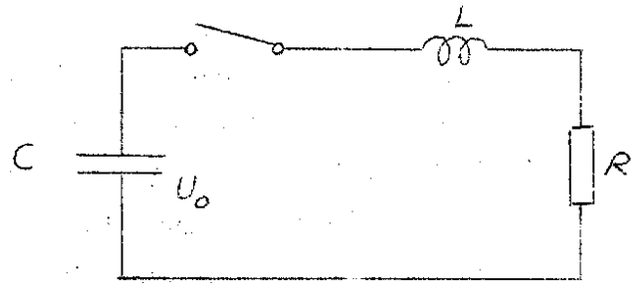

For an aperiodic discharge we have :

$$U = U_o\, e^{-\mu t}\,(1 + \mu t) \qquad ; \quad \mu = \frac{R}{2L}$$

The voltage U_o drops to 1/100 after a time

$$t_{1/100} = 6.65\,\sqrt{LC} \quad s$$

We expect to have $L \simeq 10^{-6}$ H and $C \simeq 10^{-10}$ pF. This gives :

$$t_{1/100} = 66.5 \text{ ns}$$

$$R = 200\ \Omega$$

These values are very reasonable.

Proposed solution for the vertical deflection.

The enumerated advantages of an electrostatic deflector are preponderent only if the required voltage on the electrodes can be kept in reasonable limits. At 50 MeV this is possible, especially if one adopts a solution where the electrostatic deflector serves only as 'beam switcher', i.e. merely separates the beams, the main deflection being achieved afterwards with DC bending magnets (see Ref. 1, p. 80 to 81). Such a scheme reduces the voltage and energy required in the electrostatic deflector, simplifying its circuitry. It also makes acceptable switching precision easier to obtain, because the inflence of voltage fluctuations on the electrodes decreases approximately as :

$$\frac{\alpha}{\alpha_t - \alpha}$$

α .... switching angle (produced by the electrostatic deflector)

α_t.... total required deflection angle.

In the section 3, the solution with an electrostatic beam switcher and DC bending magnets will be analysed in connection with the optics of the injection line. It will be shown that it is possible to minimise the high voltage requirements to such an extent as to be able to use medium size thyratrons as switches (in the electrode discharge circuits), the voltage being < 80 kV.

At the time, practical designs for an electrostatic beam switcher are under study*. One is considering electrostatic switchers with

a) 3 pairs of electrodes (the circuitry is simple but for maximum deflection only 2 pairs of electrodes are working).

b) 2 pairs of electrodes (all electrodes are working for maximum deflection, but the circuitry is more complicated).

3. ESTABLISHMENT OF OPTICAL CONDITIONS FOR THE INJECTION LINE

General.

The optical conditions for the injection line are defined at its input and output ends. The input to the line is taken just after the triplet IQ 21

* R.P. Featherstone, visiting scientist from University of Minnesota, Minneapolis, U.S.A.

(see Fig. 1). The output coincides with the middle of the first SI straight section (middle of 1L1). The injection line insures betatron matching of the beam and keeps it inside a chosen vacuum chamber cross section.

In addition to the conditions at input and output, some others have to be imposed in the region of the vertical deflection. This is necessary in order to minimise the high voltage requirements for the IEV.

Optical conditions at the input of the injection line.

The conditions at the input will be those needed for injection into the PS. In fact, the triplet IQ 21 is the last adjustable focusing element before the PS. So, the PS acceptance in the middle of ss 26 is transformed back to the output of IQ 21 and this gives our input conditions (see Ref. 2).

One has to take into account that the DC bending magnet IB 11 with inclined end faces will be replaced by a pulsed bending magnet IB 1, having parallel end faces. The focusing between IQ 21 and PS will therefore be changed, i.e. one will lose some horizontal and gain some vertical focusing. The loss of the horizontal focusing is disagreable, because the beam, in order to be properly injected into the PS, will have to have an excessive width at IQ 21 (> 11 cm, the vacuum chamber diameter being $\sim$ 10 cm).

This inconvenience can be overcome by putting some shims on IB 21 , the next bending magnet for injection into the PS (see Fig. 1), thus gaining the necessary horizontal focusing and leaving the vertical situation practically unchanged. The magnet IB 21 already has its end faces inclined by 244 mrad and produces a focusing of $\delta_{21} \cong 0.054\ m^{-1}$. The shims should increase the inclination of end faces to $\sim$ 300 ÷ 330 mrad, increasing the focusing to 0.08 ÷ 0.1 m^{-1}. In Fig. 5 the horizontal input conditions are presented as a function of IB 21 focusing. Already with $\delta_{21} = 0.08\ m^{-1}$ we have the beam size at IQ 21 roughly as with the present situation, which is :

Horizontal plane	Vertical plane
$(\frac{a}{b})_H = 50.1$ m	$(\frac{a}{b})_V = 5.77$ m
$(\frac{c}{b})_H = 32.2$ m	$(\frac{c}{b})_V = 0.42$ m
$e_H = 46.24$ mm	$e_V = 13.2$ mm

The injection line will be calculated in such a way as to have a matching with all input conditions corresponding to $0.08 \leq \delta_{21} \leq 0.1\ m^{-1}$

Optical conditions at the output of the injection line.

The conditions at the middle of 1L1 (SI input) are defined as follows:

Vertical phase plane: $\left(\frac{a}{b}\right)_v = 3.5$ m

$$\left(\frac{\alpha}{b}\right)_v = 0$$

$$e_v = 10.25 \text{ m}$$

Horizontal phase plane: the optical conditions depend on the number of injected turns and are presented in Fig. 10 of ref. 3.

At SI input, the beam is in the principal axis in both phase planes.

Optical conditions in the region of the vertical deflection.

As was already mentioned, some additional conditions have to be imposed to ensure:

- small working voltage on the IEV electrodes
- small beam switching angle (increased precision)
- not too long a distance for beam separation (necessarily a lens-free region).

We shall analyse the situation with the aid of Fig. 6.

The distance d between IEV electrodes, and the switching angle α are approximately given by:

$$d = 2\,(e_{IE} + \alpha L)$$

$$\alpha = \frac{2}{l}\left(e_{IB} + \frac{s}{2}\right)$$

L ... Total IEV length

e_{IE} ... vertical beam radius at IEV output

e_{IB} ... vertical beam radius at IBV input

s ... thickness of the IBV septum, = 2 cm

We suppose that for minimum voltage on IEV, the beam will have to have a waist in the vertical plane somewhere between IEV and IBV. The growth in beam diameter after the waist is a function of the ratio $\frac{a}{b}$ and of the drift length. For a certain drift distance, there exists an optimum ratio $\frac{a}{b}$, resulting in a minimum beam size. If the drift length is l_d, the best ratio is $\frac{a}{b} = l_d$, as can easily be proved analytically. In Fig. 7 the increase in beam radius for different ratios $\frac{a}{b}$ is given as well as the beam divergence b which corresponds to the optimised $\frac{a}{b}$ (thick line).

The voltage on the IEV electrodes is proportional to the product of d . α. Therefore, we look for minima of the function

$$f(\frac{a}{b},x,L,l) = d \cdot \alpha =$$

$$= \frac{4}{l} \left[2\frac{L}{l}e_{IB}^2 + e_{IB}e_{IE} + 40\frac{L}{l}e_{IB} + 10e_{IE} + 200\frac{L}{l}\right]$$

In Fig. 8 the minima of $f(\frac{a}{b}, x, L, l)$ are presented as functions of $\frac{a}{b}$. Varying the parameters L and l we get a family of curves. The x-values shown on the curves are the waist positions corresponding to the particular minimum.

From the curves fmin we can calculate the voltage on the IEV electrodes. A certain correction has to be made to take into account that the maximum switching angle is somewhat bigger than 2α (~ 20%). The reason is the somewhat closer position of IBV11 to IEV, as seen from the sketch:

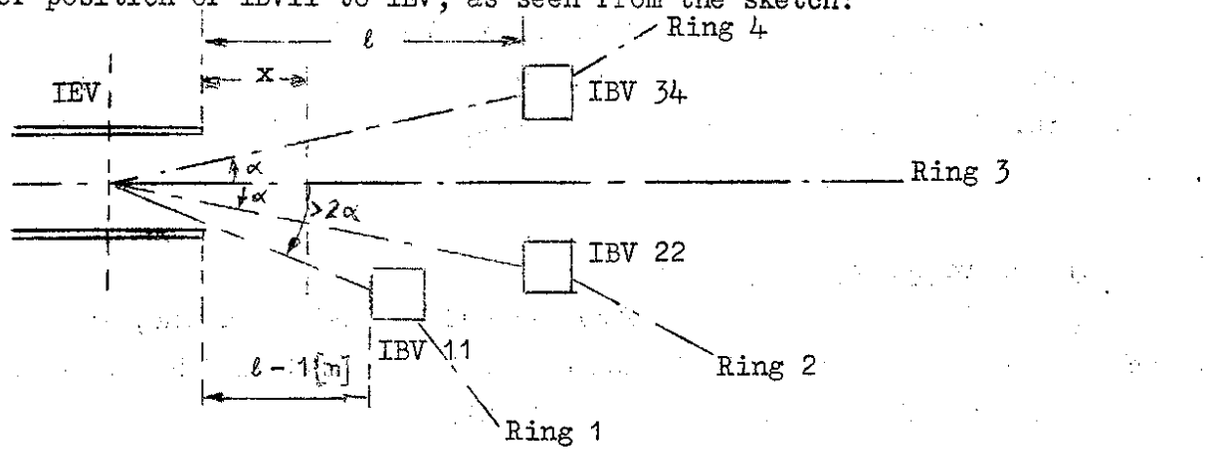

In Fig. 8a a family of curves $U = U((\frac{a}{b})_v)$ is presented for various reasonably chosen values of L and l. One sees that the best results are obtained for low values of $(\frac{a}{b})_v$ and that the condition U max < 80kV is maintained in quite a large region. However, very low values of $\frac{a}{b}$ can be undesirable from the optical point of view (small beam diameter, big divergence), as the beam will have to be transported over a certain lens-free region.

With the above calculations we know the optical conditions to be maintained in the region of the vertical deflection. This applies to the vertical phase plane. The horizontal one is not restricted.

Finally, with Fig. 9 where fmin $(\frac{a}{b}, x, L, l)$ is presented as a function of l, we have a guide for choosing a reasonable distance IEV-IBV, satisfying at the same time high voltage and beam optical requirements. These latter will be treated in the next section.

4. BEAM MATCHING IN THE TRANSVERSE PHASE PLANES

In the previous section we have established optical conditions for the injection line. It is possible now to proceed with the design itself.

In this section we treat the beam matching in both transverse phase planes.

The inclusion of optical conditions in the region of the vertical deflection splits the injection line optics into two parts:

a) IQ21 - IEV

b) IEV - SI

It is convenient to start with the second part.

All betatron matching computations are done with the aid of a programme developed in the ISR division and written by J. Barton, M. Hanney and P. Strolin. The emittance and mismatch factor presentation is according to ref. 4.

Optics in the region IEV-SI.

From IEV downstream we have four beam lines instead of one, which means that each requirement for an optical element has to be multiplied by 4. Therefore we try to put IEV as close as possible to SI.

On the sketch we show a reasonable starting arrangement of the main elements after IEV with distances chosen in agreement to functional and geometric criteria:

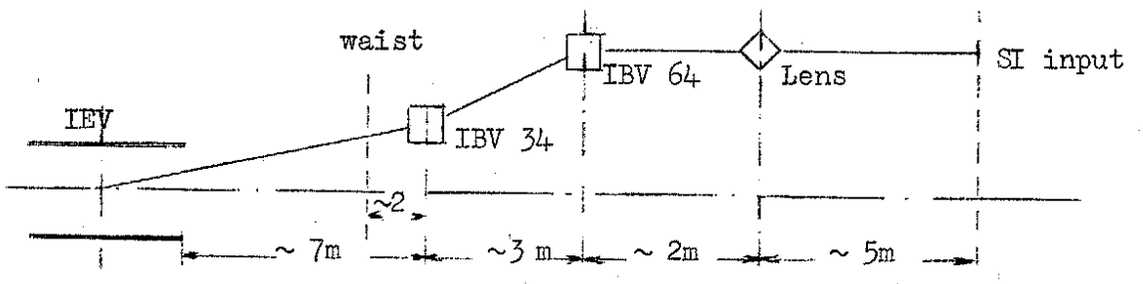

One sees that IEV has to be at roughly 17 m from SI input. The beam waist (vertical plane) is at ~ 12 m from SI. It is possible with one quadrupole put at the right position to match the beam between the waist and SI (vertically). This position of the quadrupole for various ratios $\left(\frac{a}{b}\right)_v$ at waist and various distances waist-SI is shown on Fig. 10.

Unfortunately the beam cannot be matched horizontally (the quadrupole defocuses in this plane) without having an excessive width at the waist. Therefore one has to choose as lens a quadrupole doublet which focuses in both planes. The position of the doublet does not coincide with the position of the single quadrupole. The reason is that the principal planes of a doublet are unsymmetrically placed, always on the side of the F quadrupole. In Fig. 11 the position of principal planes for 2 doublets is shown as a function of the quadrupole gradient. Only the region of interest to us is presented.

With the help of Fig. 11 one can establish approximately the position of the doublet for a vertical matching. Also one can roughly calculate the beam conditions in the horizontal plane at waist.

A short analysis was made in order to determine if the doublet has to be connected DF or FD. It proceeded as follows : the matched beam at the SI input has always in the vertical plane the emittance ellipse axis ratio $(\frac{a}{b})v = 3.5$; in the horizontal plane this ratio changes from 1.8 to 5.5, according to the number of injected turns. It would be agreeable to have to change as little as possible in focusing when passing from mono to multiturn.

To readjust only the doublet focusing would be sufficient if two things were perfectly true:

1. existence of a position before SI where all the matched beams have equal width
2. possibility of replacing the doublet with a thin lens placed at the above position.

The difference in width among the matched beams is minimum at 3.15 m in front of SI input, see Fig. 12. This means that the principal planes of the doublet for horizontal focusing have to fall approximately in this region. Consulting Fig. 11 and Fig. 1 (and noting the impossibility of placing quadrupoles closer than ~ 4 m from SI) we conclude that the doublet has to be connected DF and placed $\sim 4 \div 5$ m from SI.

With the above the optics in the region IEV-SI is sufficiently defined and it is possible to proceed with betatron matching computations.

Many cases were analysed, first separately and later in connection with the optics in the region IQ21-IEV. The results are presented in Tables 1-4 and the proposed disposition of elements is shown in Fig. 1.

Optics in the region IQ21-IEV.

Analysing this region one notices the following:

a) after IQ21, the beam is stronger focused horizontally than vertically. Therefore the first quadrupole we insert has to be a D one.

b) as seen from Fig. 1, the injection line passes through a 6 m long wall, presenting an obstacle to the insertion of elements of any kind. However, this length can be used as a drift distance necessary to separate beams of the injection and measuring line. The beam switching magnet IB2 is placed ~ 5 m before the wall in order to have enough space to install an emittance display device (see Fig. 1 and section 8). The total effective obstacle for insertion of lenses amounts therefore to 12 ÷ 13 m.

c) the last quadrupole before IEV has to be an F one, because the following horizontal waist is further away than the vertical one and also the next quadrupole is an D one.

According to a) and c) we conclude that the number of quadrupoles in this part of the injection line will be even. The matching can be achieved (several solutions were tried out, some also with uneven numbers) with a minimum of 6 quadrupoles, keeping the beam well inside a vacuum chamber of 120 mm diameter. The results are presented in tables 1-4. The proposed disposition of focusing elements is shown in Fig. 1.

5. ENERGY SPREAD REDUCTION - DEBUNCHING

The linac beam, before being injected into a circular machine, has to be debunched, i.e. its energy spread reduced.

On the sketch we represent the beam in its longitudinal phase plane:

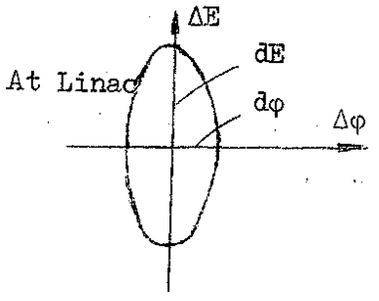

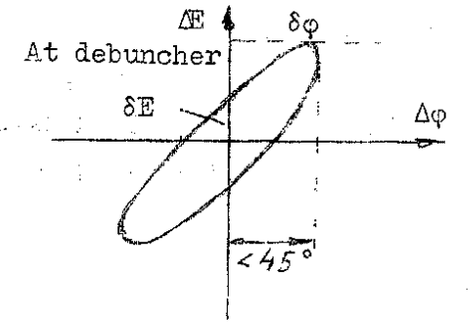

Approximately one has :

$dE.d\varphi \hat{=} \delta E.\delta\varphi$

The debuncher has a sinusoidal voltage of which only the nearly linear part is used, i.e. $-45<\varphi<45^{\circ}$ (error $<3.6\%$). At 50 MeV, 45° electrical correspond to a length of $6.25.10^{-2}$m (f = 202.56 MHz). The distance the debuncher has to be placed after the linac depends on the energy spread :

$$l_B = 6.25 \cdot 10^{-2} \frac{v}{\Delta v} \quad (m)$$

With $\frac{\Delta p}{p} = \frac{\gamma}{\gamma+1}\frac{\Delta E}{T} \simeq \frac{1}{2}\frac{\Delta E}{T}$ and $\frac{\Delta p}{p} = \frac{\Delta v}{v} + \frac{\Delta m}{m} \simeq \frac{\Delta v}{v}$;

$$l_B = 12.5 \cdot 10^{-2} \frac{T}{\Delta E} \quad (m)$$

Actually the debuncher is placed 16.5 m after the linac. The debunching possibilities are fully used (i.e. the whole nearly linear portion of the sinusoidal voltage from -45° to 45° acts on the beam) for an energy spread of

$$\frac{\Delta E}{T} = \frac{12.5}{16.5} \cdot 10^{-2} = 7.6‰ \quad \text{or}$$

ΔE = 380 keV

For a smaller energy spread, the beam bunch grows longitudinally to less than 90°, and the debuncher is not fully used. E.g. for an energy spread of $\Delta E = \pm$ 200 keV, the best debuncher position is at 31 m after the linac.

If one wishes to work always with optimum debunching efficiency regardless of the energy spread of the linac beam, one has to have two debunchers, say at 16.5 and 31 m. The working scheme is the following :

$\Delta E = \pm$ 380 keV ..... only the first debuncher is working

$|\pm 200|$ keV $< \Delta E < |\pm 380|$ keV ..... both debunchers are working

$\Delta E = \pm$ 200 keV ..... only the second debuncher is working

The installation of the second debuncher becomes less interesting if one decides that the debunching with one debuncher of a linac beam with $\Delta E < |\pm 380|$ keV is already sufficient for SI. However, it seems that to have a beam with an energy spread as low as possible is always an advantage and therefore a system with two debunchers is proposed for the injection line.

6. INJECTION INTO THE SI

For the injection proper into the SI, two types of elements are needed:

a) an electrostatic deflector IEH bending the beam to be injected by ~ 60 mrad

b) a certain number of deflection magnets ID, producing a local distortion of the closed orbit in the region of IEH.

The electrostatic deflector IEH is similar in principle to the one in straight section 26 of the PS (see Ref. 5). The working voltage is approximately:

$$U \cong \frac{\alpha \cdot d}{l} \text{ [kV]}$$

$$\cong \frac{60 \cdot 3}{1.8} = 100 \text{ kV}$$

α ... bending angle [mrad]

d ... distance between electrodes [cm]

l ... length of electrodes [m]

The number of deflection magnets ID has to be chosen according to the requirements:

Two ID's exactly half a betatron wavelength apart from each other produce:

- a local closed orbit distortion of variable amplitude
- the distorted closed orbit has zero angle at a symmetric injection point.

If one cannot place the ID's exactly $\frac{\lambda_B}{2}$ apart, a third ID is needed in order to have only a local closed orbit distortion.

If in addition one wishes to control the closed orbit angle at the point of injection (middle of 1L1), a fourth ID is needed.

A system with four ID magnets is the most general one. If possible, the ID magnets should be placed as on the following sketch:

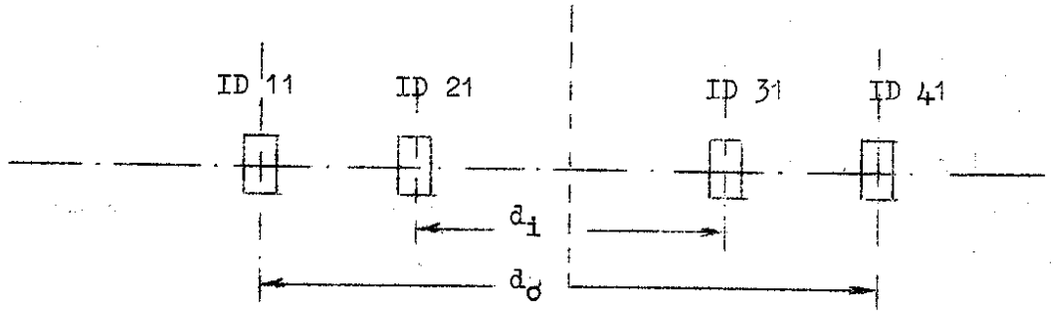

$d_i \leq \frac{1}{2} \lambda$ min ≤ 15.7 m (minimum betatron wavelength corresponds to Q max = 5)

$d_o \geq \frac{1}{2} \lambda$ max ≥ 19.625 m (maximum betatron wavelength corresponds to Q min = 4).

The arrangement is symmetric, suitable for zero injection angle.

Unfortunately the above disposition cannot be applied because the beam width becomes excessive at the position of the first SI quadrupole. It is necessary to put the ID magnets closer to IEH, shortening thus the local closed orbit distortion and bringing the beam quicker to the centre of the vacuum chamber. The position of ID's is shown on Fig. 1.

The adjustment of the four ID's can be made relatively simple. We examine the symmetric case :

1) C.O. displacement : a Σ potentiometer raises the strengths of the four ID's till the desired displacement is achieved.

2) elimination of betatron oscillation : a Δ potentiometer changes the strength of the outer two ID's with respect to the inner ones, leaving the $\Sigma \sim$ constant.

The power supplies for the ID magnets have to produce magnetic fields in the ID magnets with a variation in time like half a sinusoid. Only the $\sim$ linear, falling part of the sinusoid is used for injection. The pulse length and the intensity of the magnetic field have to be adjustable. In order to deflect a 50 MeV beam by 1 mrad, one needs 10 Gm. The maximum closed orbit displacement at IEH is $\sim$ 5 cm.

To avoid eddy-current effects, the vacuum chambers within the ID magnets should be non-metallic. It is possible to use quartz glass fused in metal flanges.

7. BEAM MEASURING LINE

Purpose

The absolute energy and the energy spread of the linac beam should be measured and controlled. A convenient technique is to pulse the linac more frequently than the SI, and during the intermediate pulses to deflect the beam into a separate beam line equipped with suitable apparatus for measuring the beam characteristics.

The deflection into the measuring line is done by a pulsed bending magnet IB2 (deflection angle ~ 70 mrad), similar to IB1 . The beam sample is taken with a vertical slit, placed in the measuring line ~ 5m downstream from IB2 (see Fig. 1).

Requirements

The energy spread of the debunched linac beam is $\leq |\pm 150|$ keV. We wish to measure it with steps of $\frac{150}{5} \div \frac{150}{3}$ keV, having as detection device a battery of Faraday cups. The step size and the distance between adjacent Faraday cups determine the momentum dispersion capacity of the measuring system.

The Faraday cup battery is under development in the linac group. The dimensions will be approximately:

cup width	~ 2mm
cup height	~ 60-70 mm
cup distance, centre to centre	~ 3mm
No. of cups	to be determined.

The system for absolute energy and energy spread measurements has to have the possibility of taking a beam sample through the whole beam width and to avoid any loss of particles in the vertical plane. Only in this way one can control the number of particles comprised in a certain $\pm\Delta E$ region.

Design

We put first down the expressions we need for the design:

a) Momentum dispersion:

$$D = \alpha L \frac{\Delta p}{p} \cong \frac{\alpha L}{2} \frac{\Delta E}{T}$$

α = nominal angle of the analysing magnet

L = distance analysing magnet - FC battery

See Fig. 13 a.

b) Resolution:

With Fig. 13 b:

$$ab = e_{MB} \cdot d \rightarrow d = \frac{ab}{e_{MB}} = \frac{E_H}{e_{MB}} ;$$

E_H = emittance of the beam sample in the horizontal phase plane.

The resolution is defined with the dispersion angle relation

$$\Delta\alpha_{min} > 2d$$

$\Delta\alpha_{min}$ corresponds to the ΔE_{min} we wish to detect.

c) Optical condition:

The slit with which the beam is sampled has to be imaged on a Faraday cup. The ratio between the cup and slit width determines the magnification:

$$M = \frac{I}{O} = \frac{\alpha_o}{\alpha_i}$$

I = image size

O = object size

See Fig. 13 c.

The momentum dispersion and resolution of a measuring system can be increased by addition of some lenses. A possible layout with four lenses is shown in Fig. 14 a. This layout keeps the desired magnification ratio $M = \frac{\alpha_o}{\alpha_I}$, but increases the beam width at the magnet MB. The consequence can be seen from the following relations :

$$D = \alpha L \frac{\Delta p}{p} = \frac{\alpha}{2} \frac{\Delta E}{T} \cdot \frac{e_{MB}}{\alpha_I}$$

$$\Delta\alpha > 2 \frac{E_H}{e_{MB}} .$$

Many systems have been considered for the measuring line. The main difficulty was to prevent beam losses in the vertical plane.

The finally chosen layout is presented on Fig. 14 b. The data are:

α[mrad]	L[m]	ℓ[m]	Dispersion for $\Delta E/T$=1‰ [mm]	Slit width[mm]	Magnification M	Number of FC's
400	9	15	5	2	1	11

The dispersion of 5 mm for $\frac{\Delta E}{T}$ = 1‰ conforms with the requirement that particles with $\Delta E = \pm 30$ keV are to be deflected into Faraday cups placed ± 3mm off the vertical centre plane. To obtain this, the beam size at the magnet MB has to be accordingly:

$$e_{MB} = \frac{2\alpha_I D}{\alpha \frac{\Delta E}{T}} = 25 \text{ mm}.$$

This e_{MB} must satisfy the resolution condition. As the emittance of the beam sample in the horizontal plane is $E_H \leq 1\ \pi \cdot 10^{-6}$ rad m, the resolution is expressed by:

$$\Delta\alpha > \frac{2}{e_{MB}} \quad \text{or} \quad e_{MB} > \frac{2}{\Delta\alpha}$$

with $\Delta\alpha = 0.12$ mrad : $\frac{2}{0.12} = 16.67 < 25$ mm.

In Fig. 14b we have drawn in the beam envelopes in both planes. At the magnet MB the beam width is < 60 mm, the height is < 50 mm.

The quadrupole gradients are also indicated. As far as the position of quadrupoles is concerned, the one of MQ 1 is not critical, the others, especially those of MQ 2 and MQ 3 are very critical.

Precision of the magnet MB

The precision required for the magnet MB depends on the accuracy with which we wish to measure the absolute energy and energy spread.

With a precision of $\pm 5 \cdot 10^{-4}$ in the integrated field, the error in the absolute energy is $\pm$ 50 keV (or 10 keV per 10^{-4} precision).

The energy spread has to be measured with a better precision. In fact, the integrated field variation across the aperture of the MB magnet can be kept $< 10^{-4}$, resulting in a ΔE error of <10 keV.

Sensitivity of the Faraday cup

The beam current contained in the sample will be $\geq$ 2.5 mA. Distributing this current on 11 FC's and taking into account that only 66.7% of particles will enter, we get for an average current in the cups :

$$I_{av} = \frac{2.5}{11} \cdot \frac{2}{3} \cong 150 \ \mu A.$$

The sensitivity should be ten times better, i.e.

$$I_{tr} \leq 15 \ \mu A.$$

The cups in development in the linac group are supposed to have a sensitivity of $\sim 10 \ \mu A$. The associated electronic circuit will be gated in order to permit enery and energy spread control at any instant during the beam pulse. The measuring time is to be $\leq 1 \ \mu s$.

8. LAYOUT OF THE INJECTION LINE

The proposed layout of the injection line is shown on Fig. 1. The setting of main elements is presented in Tables 1 to 4. If the quadrupole setting is changed by 1 ‰, the mismatch factor in both phase planes becomes ~ 1.006, i.e. the emittance increases by 6 ‰. This is negligible.

The emittance increase depends much more on the vertical deflection system. Changes of 1 ‰ in all bending angles increase the vertical emittance by 6.5 to 8%. A change of 1% in the switching angle of IEV increases the emittance by $\sim 8.5\%$.

The increase in vertical emittance due to the vertical bend (with no error) and an energy spread in the beam of $\pm$ 150 keV is $\sim 9.5\%$.

The vertical SI acceptance is approximately 30% bigger than the corresponding linac emittance.

Apart from the main elements disposed on Fig. 1 according to the computations of the previous sections, some others are also included in the layout. We shall describe them briefly.

Pick-up electrodes

Pick-up electrodes are installed in the injection line at places where the beam position in the vacuum chamber has to be controlled. They are also used to indicate the correct adjustment of the magnetic field in the IBV magnets. The error signal of the pick-up electrodes can, if wanted, be interpreted by the computer and corrections applied automatically.

TV cameras

Several TV cameras are inserted at places where the observation of the beam cross section is of interest. They are installed at the output of the vertical switcher IEV to facilitate the adjustment of the high voltage, and at the input and output of the horizontal deflector IEH to control the process of injection.

In addition some cameras are installed in the SI ring in order to show the beam position and angle with respect to the closed orbit. These cameras are placed in front of the deflection magnet ID4r and approximately one quarter of a betatron wavelength downstream.

Emittance display device

If wanted, the field in the pulsed bending magnet IB2 can be reversed and adjusted so as to deflect the beam into an emittance display device. Such a device facilitates the adjustment and the control of focusing in the injection line by offering a visual display of either the horizontal or the vertical beam emittance. The design of the device should be similar to the one presented in ref. 6, with the exception of the beam display apparatus, which is under study in the linac group. The aim is to obtain a clearer display.

Steering coils

Corrections of the beam position in the vacuum chamber are made by steering coils, which are usually installed close to observation devices such as pick-up electrodes or TV cameras. Steering coils act in pairs, i.e. two of them are needed to correct for beam deviations.

9. CONCLUSION

The injection line as it is proposed, is a possible solution to the problem of beam transport linac-SI. It is based on the choice we have made for the vertical deflection system and on conditions we have established in early sections. A perfect betatron matching is ensured for a large range of input conditions and for injection of one up to ten turns. The two debuncher system should meet the requirements for a low energy spread. Beam observing and measuring devices should facilitate the operation.

An operational facility is also the fact that the quadrupoles IQ7 and IQ8 are very efficient when changing the number of injected turns. With the line adjusted for a 4-turn injection, one achieves a monoturn injection with mismatch factors of 1.039 (horizontally) and 1.058 (vertically) and a 10-turn injection with 1.14 resp. 1.02, by changing only the focusing of IQ7 and IQ8. It is obvious that the mismatch factors are much more favourable when the change in injected turns is not so drastic.

Concluding, we would like to stress again that the proposed injection line is based on certain conditions. A change in these conditions or an inclusion of others might result in modifications of the presented layout.

Distribution

Linac Scientific Staff
List MPS/SI 1

References

1) Study Group for CPS Improvements, The Second Stage CPS Improvement Study, MPS/Int. DL/B 67-19.

2) P. Têtu, Adaptation du faisceau linac au PS, MPS/Int. Lin 66-1.

3) L. Nielsen, Investigation of the Possibilities of Multiturn Injection into the Booster, MPS/Int. Lin 67-8.

4) H.G. Hereward, The Properties of Particle Beams in Optical Matching Systems in Terms of Phase-Plane Ellipso-Shapes, PS/Int. TH 59-5.

5) E. Boltezar, Electrostatic Inflector in Straight Section 26 of PS, MPS/ML Note 68-8.

6) Th.J.M. Sluyters, R. Damm, A. Otis, A Simple Pulse Transverse Phase Space Beam Analyzer, B.N.L. Report.

A P P E N D I X I

ESTIMATE OF THE SPACE CHARGE INFLUENCE

ON THE BEAM ALONG A DRIFT LENGTH

If one tries to get some general expressions concerning space charge action, many simplifications have to be made.

At the start we make two assumptions :

- the beam has a rotational symmetry,
- there is only a radial field component, so the problem is a one-dimensional one (the fact that the linac beam is bunched will be taken into account later as a correction).

The starting equations are :

Equation of motion : $$m \frac{d\vec{v}}{dt} = q \vec{E} \qquad (1)$$

Equation of continuity : $$\nabla (\rho \vec{v}) = - \frac{\delta \rho}{\delta t} \qquad (2)$$

Poisson's equation : $$\nabla \vec{E} = \frac{\rho}{\epsilon} \qquad (3)$$

The notation in the formulae is usual. All the terms are functions of time and space (only r coordinate).

With (2) + $\frac{\delta}{\delta t}$ (3) we get :

$$\nabla \frac{\delta \vec{E}}{\delta t} + \frac{1}{\epsilon} \nabla (\rho \vec{v}) = 0 \qquad \text{or}$$

$$\nabla \left\{ \frac{\delta \vec{E}}{\delta t} + \frac{1}{\epsilon} \rho \vec{v} \right\} = 0$$

The terms in the brackets represent the displacement and conduction current. It is easy to see that in our case their sum must be zero, i.e.

$$\frac{\delta \vec{E}}{\delta t} = - \frac{1}{\epsilon} \rho \vec{v} \tag{4}$$

We apply the operators ∇ and $\frac{\delta}{\delta t}$ on equ. (1) :

$$\nabla \frac{d\vec{v}}{dt} = \frac{q}{m} \nabla \vec{E} = \frac{q}{m} \frac{\rho}{\epsilon} \tag{5}$$

$$\frac{\delta}{\delta t} \frac{d\vec{v}}{dt} = \frac{q}{m} \frac{\delta \vec{E}}{\delta t} = - \frac{q}{m} \frac{1}{\epsilon} \rho \vec{v} \tag{6}$$

with $\vec{v}$.(5) + (6) we have :

$$\vec{v} \left(\nabla \frac{d\vec{v}}{dt} \right) + \frac{\delta}{\delta t} \frac{d\vec{v}}{dt} = 0 \tag{7}$$

$\frac{d\vec{v}}{dt}$ is the acceleration $\vec{a}$. The acceleration of particles due to space charge forces is a function of time and position. The total derivative is therefore :

$$\frac{d\vec{a}}{dt} = \frac{\delta \vec{a}}{\delta t} + (\vec{v} \nabla) \vec{a}$$

Introducing this into (7) we get :

$$\frac{d\vec{a}}{dt} - (\vec{v} \nabla) \vec{a} + \vec{v} (\nabla \vec{a}) = 0 \qquad \text{or}$$

$$\frac{d\vec{a}}{dt} = (\vec{v} \nabla) \vec{a} - \vec{v} (\nabla a) \tag{7'}$$

If the motion is only radial, we can write :

$$\vec{a} = \varphi (r,t) \vec{r}$$
$$\vec{v} = \psi (r,t) \vec{r}$$

Putting this into (7') :

$$(\vec{v}\nabla)\,\vec{a} \;-\; \vec{v}\,(\nabla\vec{a}) \;=\; \psi\, r\,\frac{\delta}{\delta r}\,(\varphi\vec{r}) \;-\; \psi\,\vec{r}\,\left(2\varphi + r\,\frac{\delta\varphi}{\delta r}\right) \;=$$

$$= \left\{ \psi\, r\,\frac{\delta\varphi}{\delta r} + \psi\,\varphi \;-\; 2\psi\,\varphi - \psi\, r\,\frac{\delta\varphi}{\delta r} \right\}\vec{r} \;=$$

$$= \;-\,\psi\,\varphi\,\vec{r} \;=\; -\,\frac{(\vec{v}\,\vec{a})}{r^2}\;\vec{r}$$

Finally (7') becomes :

$$\frac{d\vec{a}}{dt} + \frac{(\vec{a}\,\vec{v})}{r^2}\;\vec{r} \;=\; 0 \qquad (8)$$

As the motion is only radial :

$$\vec{v} \;=\; \frac{d\vec{r}}{dt} \;=\; \dot{r}\,\vec{r} \qquad ;\quad \dot{r} = \frac{dr}{dt}$$

$$\vec{a} \;=\; \ddot{r}\,\vec{r} \qquad ;\quad \ddot{r} = \frac{d^2r}{dt^2}$$

$$\frac{d\vec{a}}{dt} \;=\; \dddot{r}\,\vec{r} \qquad ;\quad \dddot{r} = \frac{d^3r}{dt^3}$$

Equation (8) can be written in the form :

$$\dddot{r} + \frac{\ddot{r}\,\dot{r}}{r} \;=\; 0 \qquad \text{or}$$

$$\dot{r}\left\{ \frac{\dddot{r}}{\ddot{r}} + \frac{\dot{r}}{r} \right\} = \dot{r}\,\frac{d}{dt}\,\ln(\dot{r}\,r) \;=\; 0 \qquad (9)$$

The solution of (9) :

$$\dot{r}\,r \;=\; K(r)$$

$$\dot{r} \;=\; \frac{K(r)}{r} \qquad (10)$$

This is the differential equation of motion we were looking for. K , in general, is a function of r and depends on initial conditions.

It is easy to show that K is a constant only in the case the space charge density $\rho(r) = \text{const.} = \rho_o$. If the initial beam radius is r_o (at $t = 0$), we have :

$$r_o = \frac{q}{m} E_{r_o} = \frac{K}{r_o}$$

Putting in the expression for the radial electric field, E_{r_o}, K becomes :

$$K = \frac{q}{2m\epsilon_o} \rho_o r_o^2 \qquad (11)$$

Multipling (10) with $\dot{r}$ we get :

$$\dot{r}\,\ddot{r} = K \frac{\dot{r}}{r} \qquad \text{or}$$

$$\frac{1}{2} \frac{d}{dt} (\dot{r}^2) = K \frac{d}{dt} \ln r \qquad (12)$$

To integrate (12) we must choose initial conditions :

$$\text{at } t = 0 \rightarrow \begin{matrix} r = r_o \\ \dot{r} = 0 \end{matrix}$$

$$\frac{1}{2} \dot{r}^2 = K (\ln r - \ln r_o) \qquad \text{or with (11)}$$

$$\left(\frac{d}{dt} \frac{r}{r_o} \right)^2 = \frac{2\rho_o}{m\,\epsilon_o} \ln \frac{r}{r_o} = K_1^2 \ln \frac{r}{r_o} \qquad (13)$$

We introduce a new, dimensionless variable $x = \frac{r}{r_o}$ and write (13) as :

$$\frac{\dot{x}}{x} = K_1 \sqrt{\ln x} \qquad \text{or}$$

$$\int_1^x \frac{dx}{\sqrt{\ln x}} = K_1 t \qquad (13')$$

With the substitution $x = e^{\xi^2}$, $dx = 2\xi\, e^{\xi^2} d\xi$, the above integral is put into the form :

$$2 \int_0^{\sqrt{\ln x}} e^{\xi^2} d\xi = K_1 t$$

This is the Gauss integral, which is tabulated (e.g. in Jahnke-Emde: Tafeln Höherer Funktionen).

In (13') we have the time expressed in terms of beam radius. What we wish, in fact, is the inverse function, i.e. the beam radius presented as function of time (or of drift length) :

$$x = \frac{r}{r_0} = \Phi (K_1 t) \quad \text{or}$$

$$\vec{r} = \vec{r}_0 \; \Phi \; (K_1 t)$$

Differentiating $\vec{r}$ with respect to t, we get $\dot{\vec{r}}$ of the form :

$$\dot{\vec{r}} = \varphi (t) \; \vec{r}$$

The velocity of the particle is only a function of time. The position, at $t = 0$, is included in $\varphi(t)$. All the particles with the same initial position have the same velocity. This means that our analysis is consistent only assuming zero emittance.

Differentiating again we get $\ddot{\vec{r}}$ of the form :

$$\ddot{\vec{r}} = \psi (t) \; \vec{r} \qquad \text{or}$$

$$\vec{E} = \frac{m}{q} \; \psi (t) \; \vec{r}$$

With the Poisson equation :

$$\rho = \epsilon_0 \; \nabla \vec{E} = \frac{m}{q} \; \epsilon_0 \; \nabla (\psi \; \vec{r})$$

After some calculations one obtains :

$$\rho = \frac{\rho_0}{\Phi^2 (K_1 t)}$$

ρ is not function of r, or, in other words, a uniform charge density remains uniform if zero emittance is assumed.

It remains now to analyse the factor K_1, in the equation (13') which depends on the beam current :

$$K_1 = \sqrt{\frac{q}{m\,\epsilon_0}\,\rho_0} = \sqrt{\frac{q}{m\,\epsilon_0}\,\frac{I}{v_p . v_0^2\,\pi}} = 1.81 \cdot 10^5\,\frac{\sqrt{I}}{r_0} \qquad (14)$$

(14) is a numerical relation valid for a 50 MeV beam. I is to be given in mA, r_0 in cm. It is important to decide what value to put for I in (14) because the beam is bunched. In Fig. 3 are sketched the beam bunches before and after the debunching process. We have decided to put for I the following :

$$I = I_0\,\frac{D}{d}\,K_2$$

I_0 ..... linac current
K_2 ..... correction factor
$\frac{D}{d}$ ..... bunching factor.

The correction factor K_2 takes into account that between bunches there are regions with zero current. If we calculate the radial field of a finite line charge and compare the results with an infinite line, then the ratio of electric fields in both cases is our correction factor K_2 :

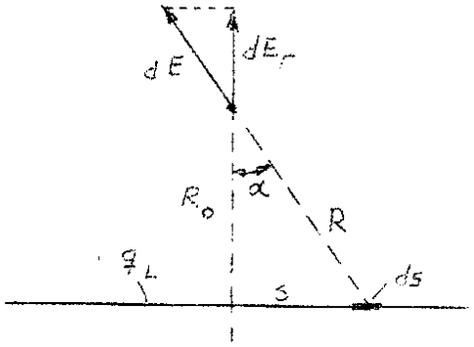

q_L ..... line charge density

$$s = R_0 \operatorname{tg} \alpha$$
$$ds = R_0(1 + \operatorname{tg}^2\alpha)\,d\alpha$$
$$R = \frac{R_0}{\cos \alpha}$$

$$dE_r = \frac{q_L \cdot ds}{4\pi\,\epsilon_0} \cdot \frac{1}{R^2} \cos \alpha = \frac{q_L}{4\pi\,\epsilon_0 R_0} (1 + \operatorname{tg}^2\alpha) \cos^2 \alpha \; d\alpha$$

$$E_r = 2 \int_0^{\alpha} dE_r = \frac{q_L}{2\pi \epsilon_0 R_0} \underbrace{\int_0^{\alpha} (1 + tg^2\alpha) \cos^2\alpha \; d\alpha}_{= \sin \alpha}$$

Finally :

$$E_r = \frac{q_L}{2\pi \epsilon_0 R_0} \sin \alpha$$

If the beam were continuous, the radial field would be given with :

$$E_r = \frac{q_L}{2\pi \epsilon_0 R_0}$$

The correction factor K_2 is therefore :

$$K_2 = \sin \alpha \qquad \text{or}$$

$$I = I_0 \frac{D}{d} \sin \alpha$$

In Fig. 4 we have presented the result of the above analysis. The ratio $\frac{r}{r_0}$ is given as function of drift distances before and after debunching ($\frac{D}{d}$ = 20 resp.4) The presented curve is valid for I_0 = 100 mA and r_0 = 1 cm, but for other I and r a scaling factor is indicated on the diagram.

TABLE I (MONOTURN INJECTION)

Quadrupoles : aperture 120 mm ∅
length 0.5 m

Input conditions H	Input conditions V	Output conditions H	Output conditions V	Mismatch factor H	Mismatch factor V
13.330 -j27.950	5.77 -j0.42	5.5 j0	3.5 j0	1	1

Element	K[m^{-2}]	Magn. grad. G/cm	Beam width [mm] Input	Beam width [mm] Output	Beam height [mm] Input	Beam height [mm] Output
IQ1	0.16779	~ 17	56.82	56.96	69.40	70.04
IQ2	0.12890	~ 13	75.50	75.80	60.50	60.82
IQ3	0.12711	~ 13	62.90	63.14	82.02	82.20
IQ4	0.09987	~ 10	87.20	87.50	63.24	63.08
IQ5	0.37991	~ 38	66.00	70.70	86	82.84
IQ6	0.35910	~ 36	94.80	96.50	54.24	49.48
IQ7r	0.98563	~ 99	22.45	25.12	54.47	50.33
IQ8r	0.91503	~ 92	30.94	33.20	39.72	33.38

Input conditions H	Input conditions V	Output conditions H	Output conditions V	Mismatch factor H	Mismatch factor V
18.90 -j28.44	5.77 -j0.42	5.5 j0	3.5 j0	1	1

IQ1	0.17378	~ 17	59.18	59.72	69.40	70.00
IQ2	0.14534	~ 15	84.70	85.12	59.12	59.40
IQ3	0.13374	~ 13	69.24	69.42	82.22	82.44
IQ4	0.10255	~ 10	94.64	94.88	62.80	62.62
IQ5	0.37728	~ 38	69.05	71.56	85.48	82.38
IQ6	0.35115	~ 35	94.88	96.50	54.18	49.48
IQ7r	0.98563	~ 99	22.45	25.12	54.47	50.33
IQ8r	0.91503	~ 92	30.94	33.20	39.72	33.38

Input conditions H	Input conditions V	Output conditions H	Output conditions V	Mismatch factor H	Mismatch factor V
26.43 -j26.13	5.77 -j0.42	5.5 j0	3.5 j0	1	1

IQ1	0.17363	~ 17	61.52	62.44	69.40	70.00
IQ2	0.15881	~ 16	92.76	93.28	59.14	59.60
IQ3	0.14275	~ 14	74.04	74.14	85.36	85.62
IQ4	0.10523	~ 11	100.66	100.86	63.96	63.70
IQ5	0.37201	~ 37	70.08	72.40	85.00	81.92
IQ6	0.34327	~ 34	94.98	96.50	54.14	49.48
IQ7r	0.98563	~ 99	22.45	25.12	54.47	50.33
IQ8r	0.91503	~ 92	30.94	33.20	39.72	33.38

TABLE II (4-TURN INJECTION)

Quadrupoles : aperture 120 mm ∅
length 0.5 m

Input conditions H	Input conditions V	Output conditions H	Output conditions V	Mismatch factor H	Mismatch factor V
13.33 -j27.95	5.77 -j0.42	2.8 j0	3.5 j0	1	1

Element	K[m^{-2}]	Magn. grad. G/cm	Beam width [mm] Input	Beam width [mm] Output	Beam height [mm] Input	Beam height [mm] Output
IQ1	0.16879	~ 17	56.82	56.96	69.40	70.04
IQ2	0.11956	~ 12	75.70	76.08	60.26	60.51
IQ3	0.11982	~ 12	65.88	62.28	79.28	79.42
IQ4	0.10932	~ 11	92.74	93.00	62.00	61.98
IQ5	0.38402	~ 38	66.33	68.74	90.90	87.66
IQ6	0.35385	~ 35	91.44	93.02	57.60	52.56
IQ7r	1.06514	~107	23.01	26.13	57.90	52.94
IQ8r	1.10356	~110	32.71	34.69	40.56	33.38

Input conditions H	Input conditions V	Output conditions H	Output conditions V	Mismatch factor H	Mismatch factor V
18.90 -j28.44	5.77 -j0.42	2.8 j0	3.5 j0	1	1

IQ1	0.17849	~ 18	59.18	59.76	69.40	69.96
IQ2	0.13842	~ 14	85.62	86.18	58.04	58.22
IQ3	0.12493	~ 12	72.96	73.28	77.90	78.06
IQ4	0.11101	~ 11	100.71	100.88	60.82	60.84
IQ5	0.38234	~ 38	61.40	69.50	90.32	87.15
IQ6	0.34563	~ 35	91.52	93.02	57.44	52.56
IQ7r	1.06514	~107	23.01	26.13	57.90	52.94
IQ8r	1.10356	~110	32.71	34.69	40.56	33.38

Input conditions H	Input conditions V	Output conditions H	Output conditions V	Mismatch factor H	Mismatch factor V
26.43 -j26.13	5.77 -j0.42	2.8 j0	3.5 j0	1	1

IQ1	0.16691	~ 17	61.52	62.38	69.40	70.05
IQ2	0.15962	~ 16	91.30	91.80	60.70	61.28
IQ3	0.14244	~ 14	71.66	71.65	89.70	90.04
IQ4	0.10228	~ 10	95.66	95.82	68.50	68.26
IQ5	0.36992	~ 37	67.42	69.70	90.40	87.09
IQ6	0.34466	~ 35	91.54	93.02	57.52	52.56
IQ7r	1.06514	~107	23.01	26.13	57.90	52.94
IQ8r	1.10356	~110	32.71	34.69	40.56	33.38

TABLE III (10-TURN INJECTION)

Quadrupoles : aperture 120 mm ø
length 0.5 m

Input conditions H	Input conditions V	Output conditions H	Output conditions V	Mismatch factor H	Mismatch factor V
13.33	5.77	1.8	3.5	1	1
-j27.95	-j0.42	j0	j0		

Element	K[m^{-2}]	Magn. grad G/cm	Beam width [mm] Input	Beam width [mm] Output	Beam height [mm] Input	Beam height [mm] Output
IQ1	0.17202	~ 17	56.82	56.98	69.40	70.00
IQ2	0.14299	~ 14	76.32	76.51	59.52	59.88
IQ3	0.12546	~ 13	60.08	60.02	82.76	83.04
IQ4	0.10122	~ 10	78.30	78.41	66.16	66.16
IQ5	0.38298	~ 38	57.48	59.74	94.14	90.70
IQ6	0.36161	~ 36	80.14	81.58	59.32	54.10
IQ7r	1.10107	~110	25.58	29.54	59.58	54.20
IQ8r	1.19476	~119	37.44	39.57	40.96	33.38

Input conditions H	Input conditions V	Output conditions H	Output conditions V	Mismatch factor H	Mismatch factor V
18.90	5.77	1.8	3.5	1	1
-j28.44	-j0.42	j0	j0		

IQ1	0.16394	~ 16	59.18	59.64	69.40	70.08
IQ2	0.15370	~ 15	82.74	82.98	61.38	61.98
IQ3	0.13989	~ 14	63.60	63.50	90.14	90.49
IQ4	0.10467	~ 10	83.60	83.90	69.34	69.16
IQ5	0.37394	~ 37	58.58	60.66	93.48	90.06
IQ6	0.35142	~ 35	80.24	81.60	59.26	54.10
IQ7r	1.10107	~110	25.58	29.54	59.58	54.20
IQ8r	1.19476	~119	37.44	39.57	40.96	33.38

Input conditions H	Input conditions V	Output conditions H	Output conditions V	Mismatch factor H	Mismatch factor V
26.43	5.77	1.8	3.5	1	1
-j26.13	-j0.42	j0	j0		

IQ1	0.17113	~ 17	61.52	62.42	69.40	70.00
IQ2	0.16823	~ 17	92.24	92.64	59.72	60.28
IQ3	0.14241	~ 14	69.92	69.72	89.06	89.46
IQ4	0.10356	~ 10	89.70	89.70	68.80	68.62
IQ5	0.37126	~ 37	59.48	61.38	92.90	89.54
IQ6	0.34341	~ 34	80.32	81.58	59.20	54.10
IQ7r	1.10107	~110	25.58	29.54	59.58	54.20
IQ8r	1.19476	~119	37.44	39.57	40.96	33.38

TABLE IV

Vertical electrostatic deflector, IEV, with two pairs of electrodes:

Length [m]		2
Distance between electrodes [mm]		~ 76
α max [mrad]		~ 17
HV EV		~ 65
Beam width [mm]	input	~ 88
	output	~ 70
Beam height [mm]	input	~ 46
	output	~ 40

Vertical bending magnets IBV:

Element	α [mrad]	Beam width [mm]	Beam height [mm]
IBV 11	~ 90	$\leq$ 60	$\leq$ 40
IBV 22	~ 57	$\leq$ 60	$\leq$ 40
IBV 34	~ 57	$\leq$ 60	$\leq$ 40
IBV 41	~106	$\leq$ 40	$\leq$ 60
IBV 52	~ 65	$\leq$ 40	$\leq$ 60
IBV 64	~ 65	$\leq$ 40	$\leq$ 60

FIG. 1: Proposed layout of the injection line

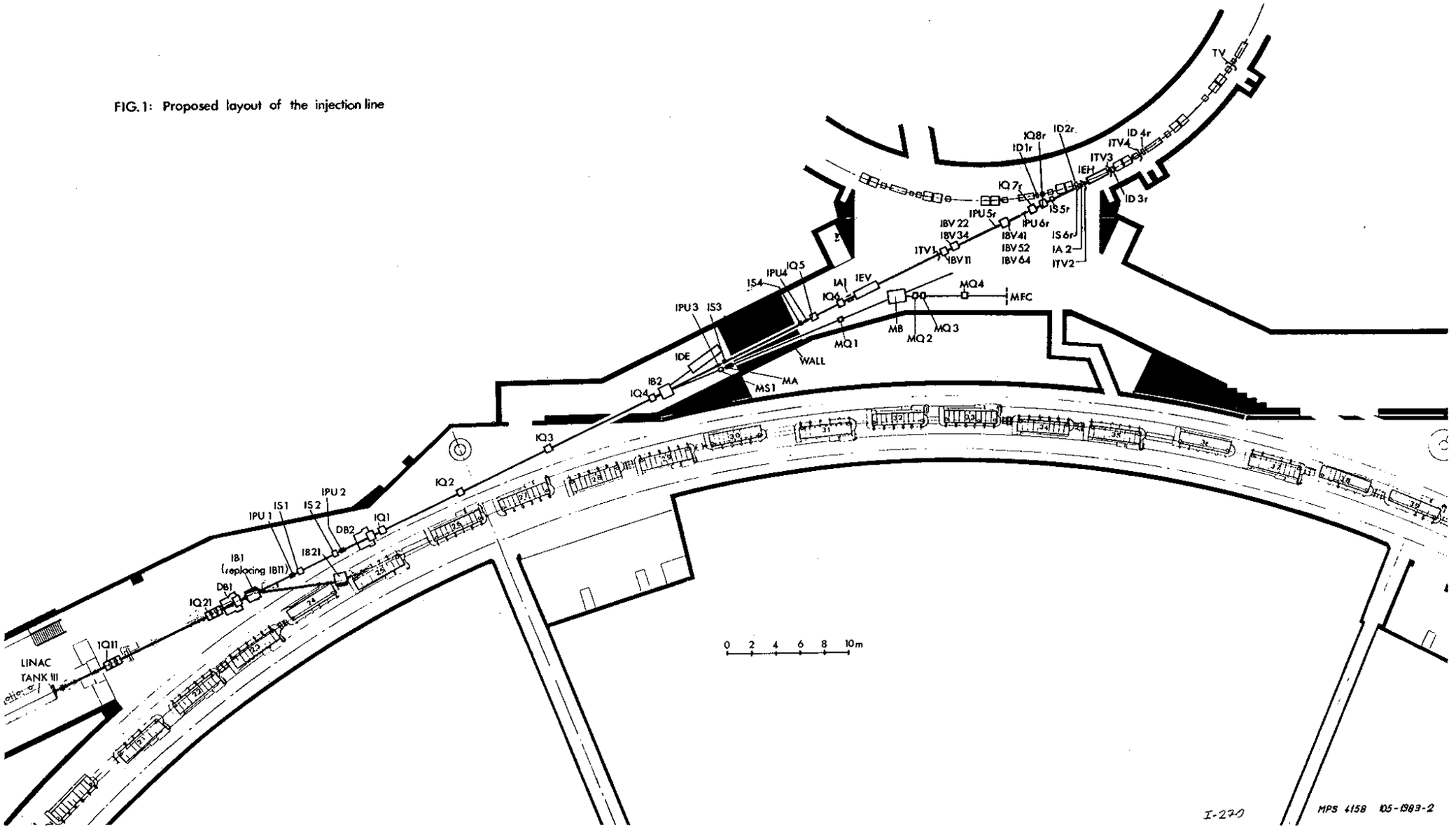

FIG. 2 : Typical curve I=f(E) for the linac beam
(50 MeV duoplasmatron ion source)

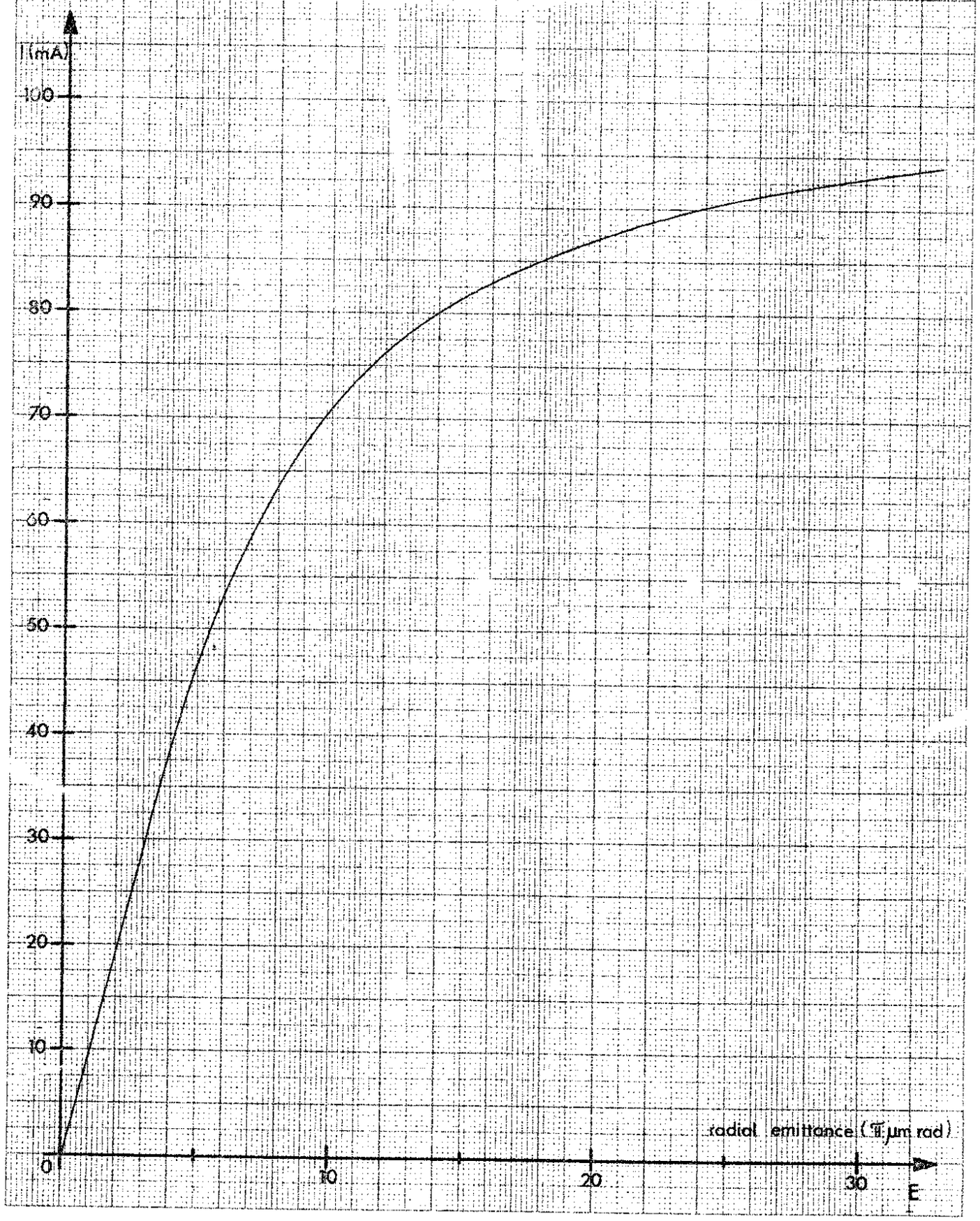

FABRICATION SUISSE

8.5.68

FIG. 3: RF structure of the linac beam

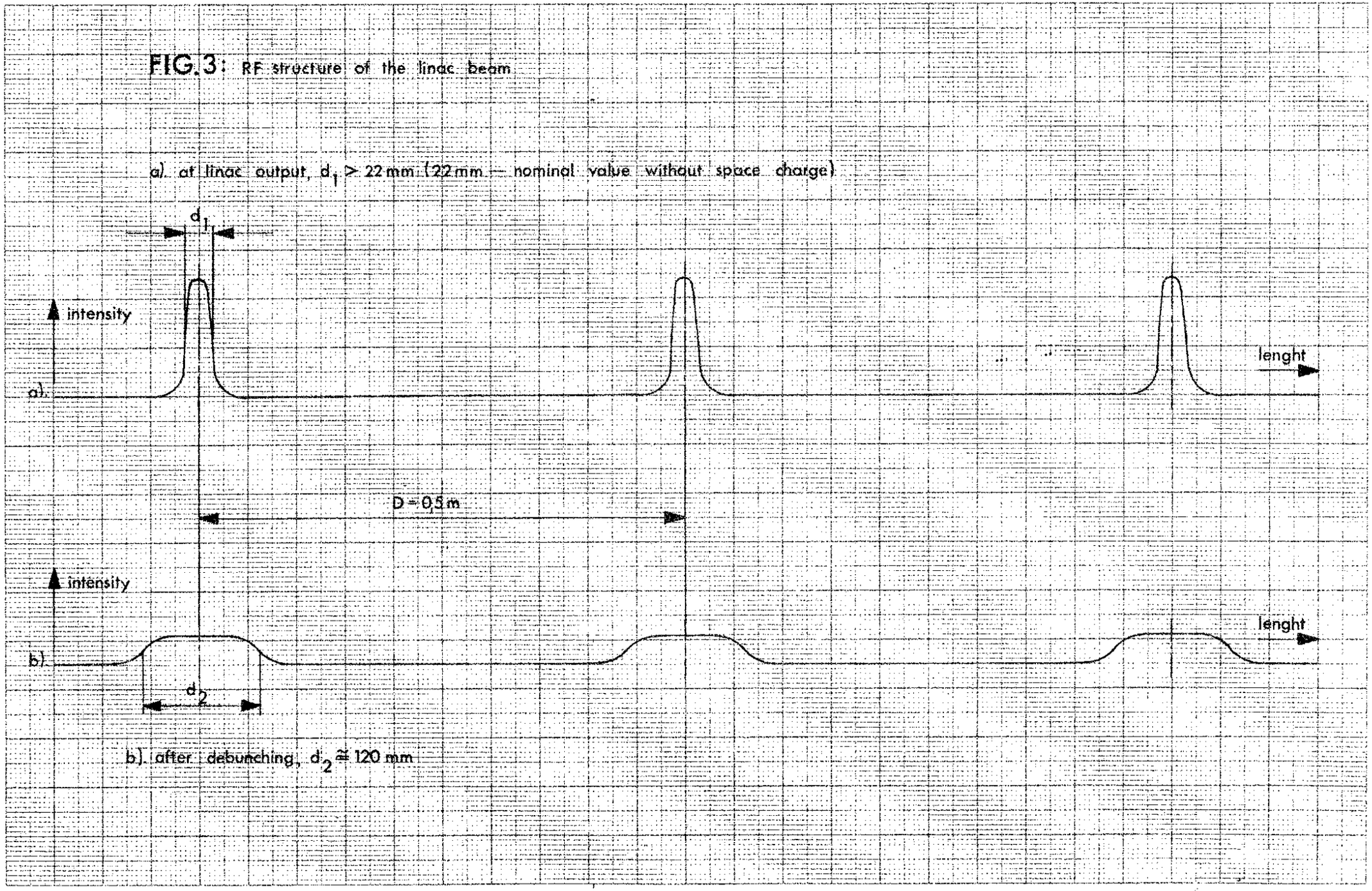

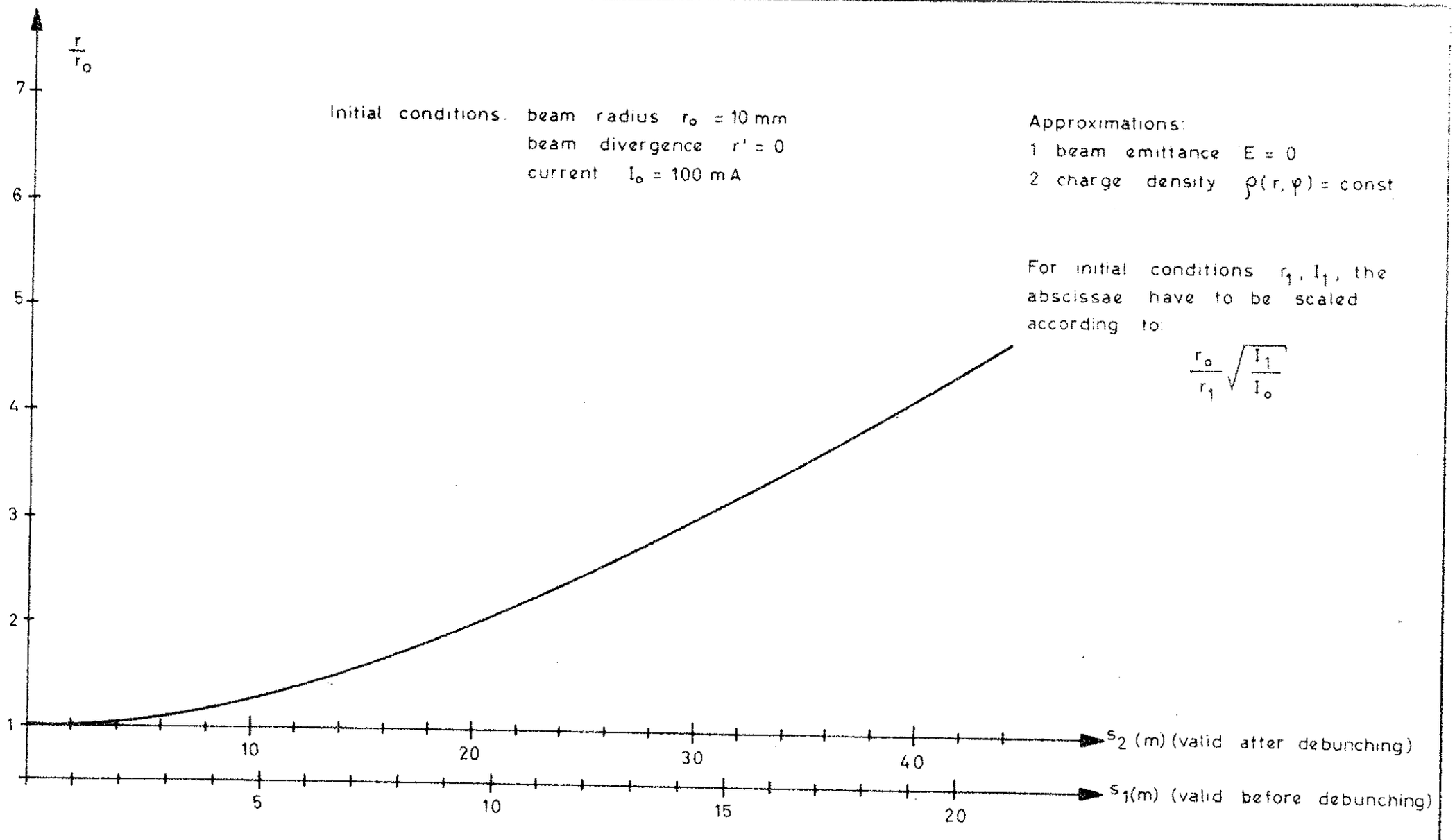

FIG. 4: Beam spreading due to space charge action

FIG. 5 : Optical conditions (horizontal phase plane) at output of IQ 21 as function of IB 21 focusing (with additional shims)

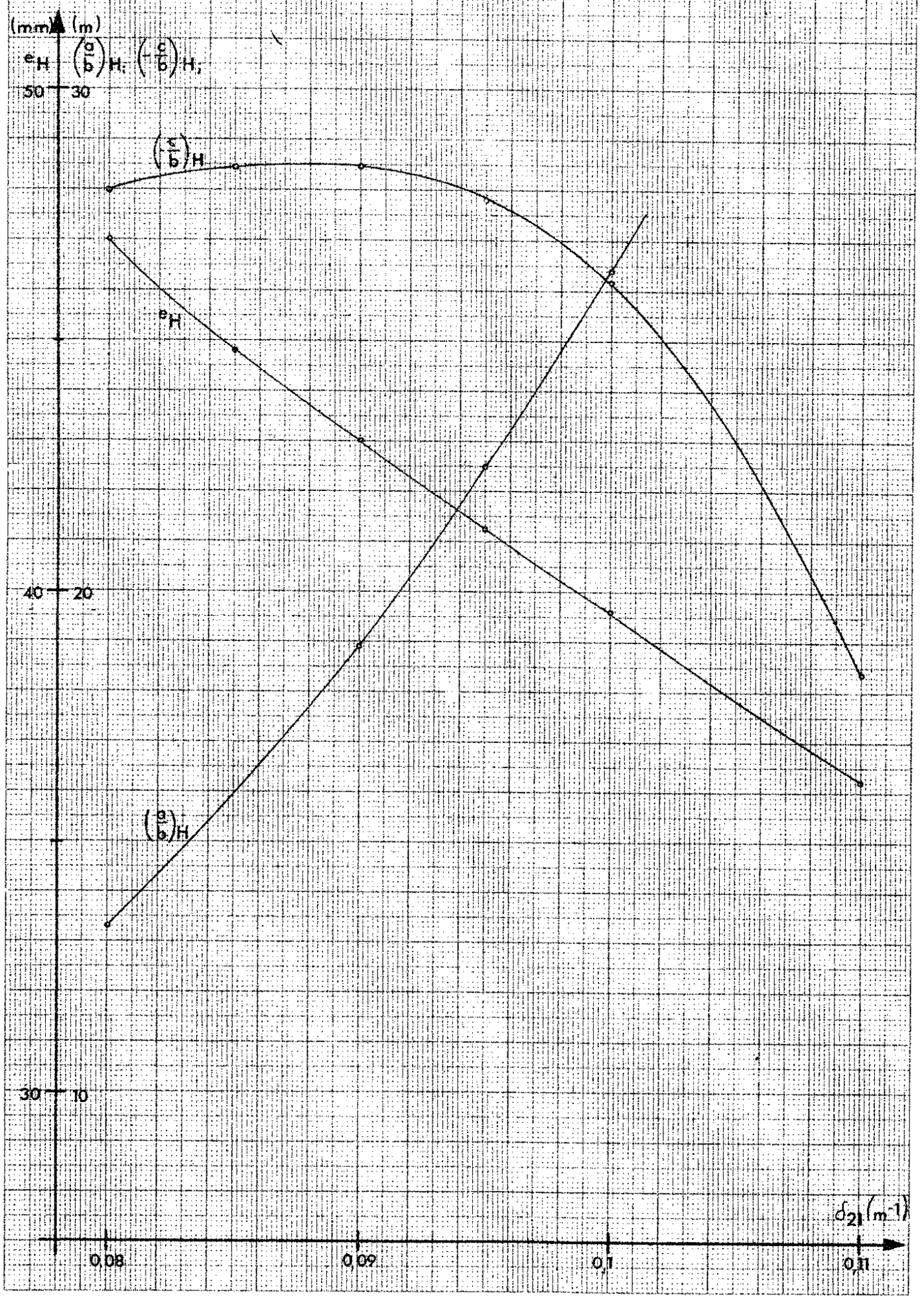

FABRICATION SUISSE

30.4.68

FIG. 6 : Optimization of beam optical conditions (vertical phase plane) in the region of the vertical switcher IEV

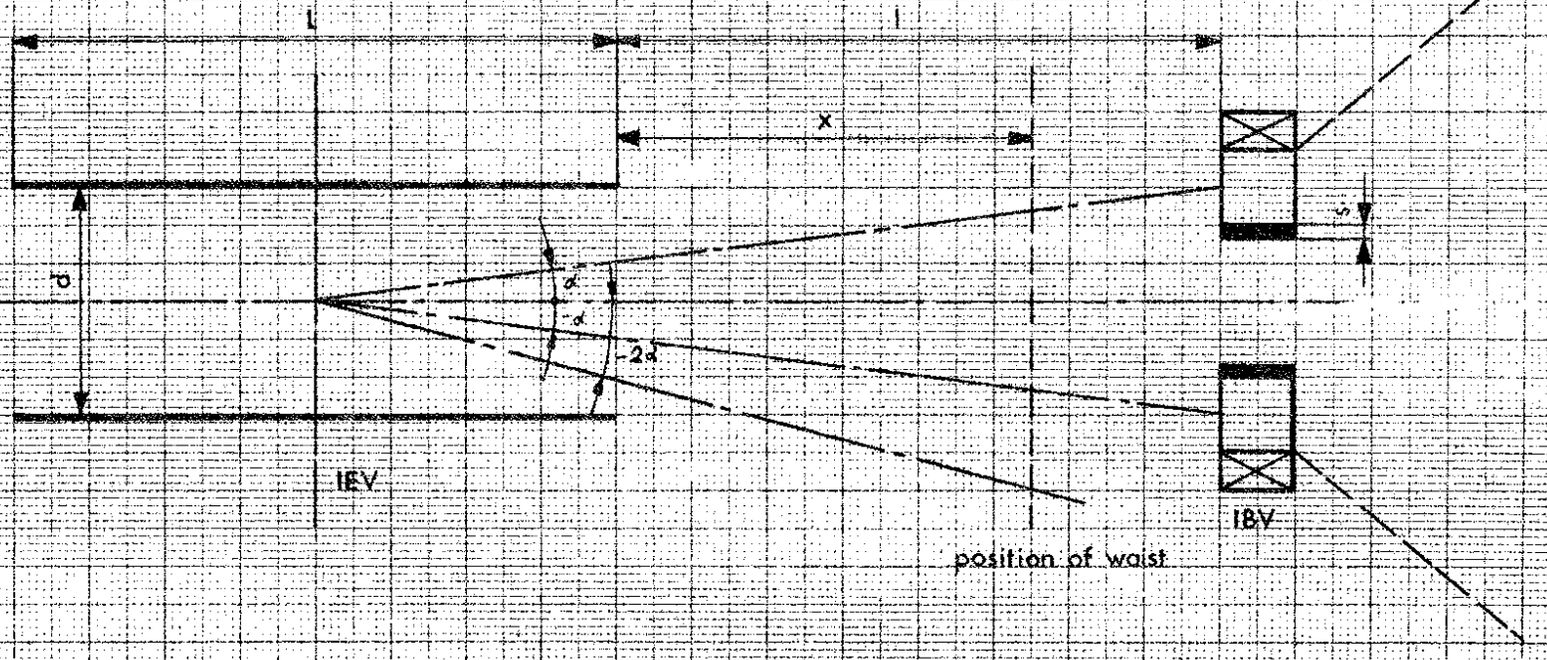

FIG. 7: Beam radius as function of drift lenght for various values of $\frac{a}{b}$

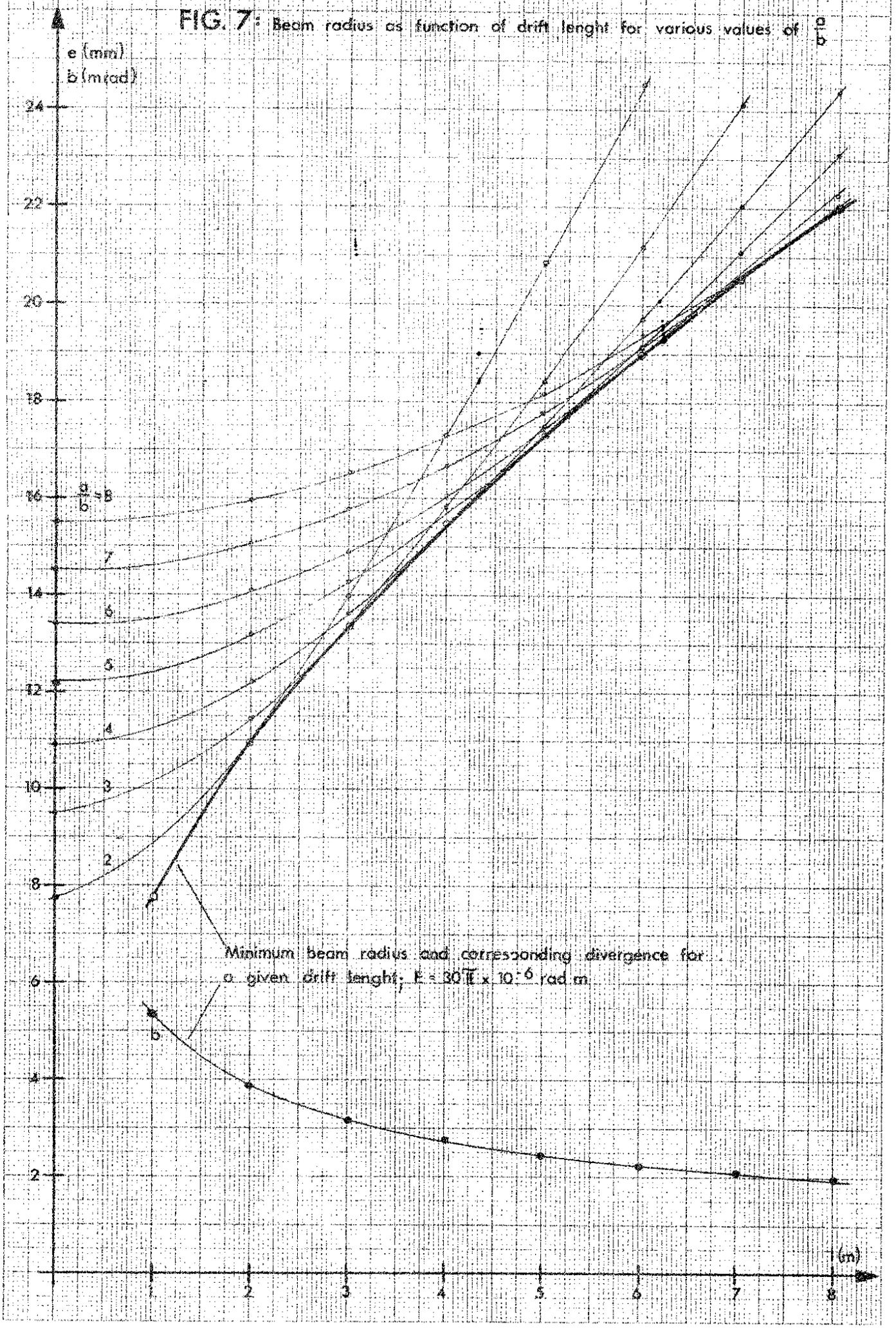

FABRICATION SUISSE

30.4.68

FIG. 8 : Minima of $f\left(\frac{a}{b}, x, L, l\right)$ as function of $\frac{a}{b}$. The position of waist corresponding to f min is indicated. L and l are parameters.

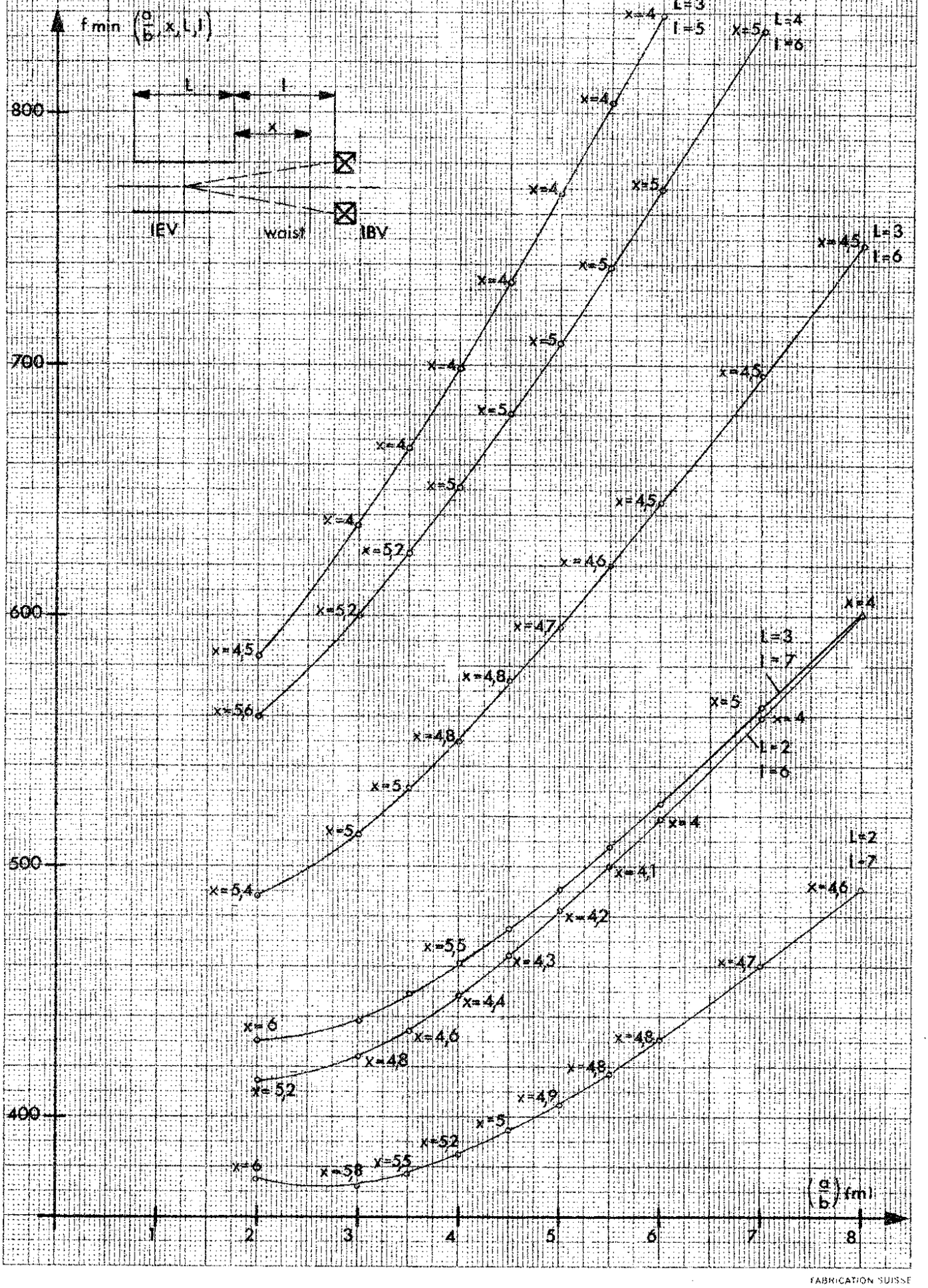

FABRICATION SUISSE

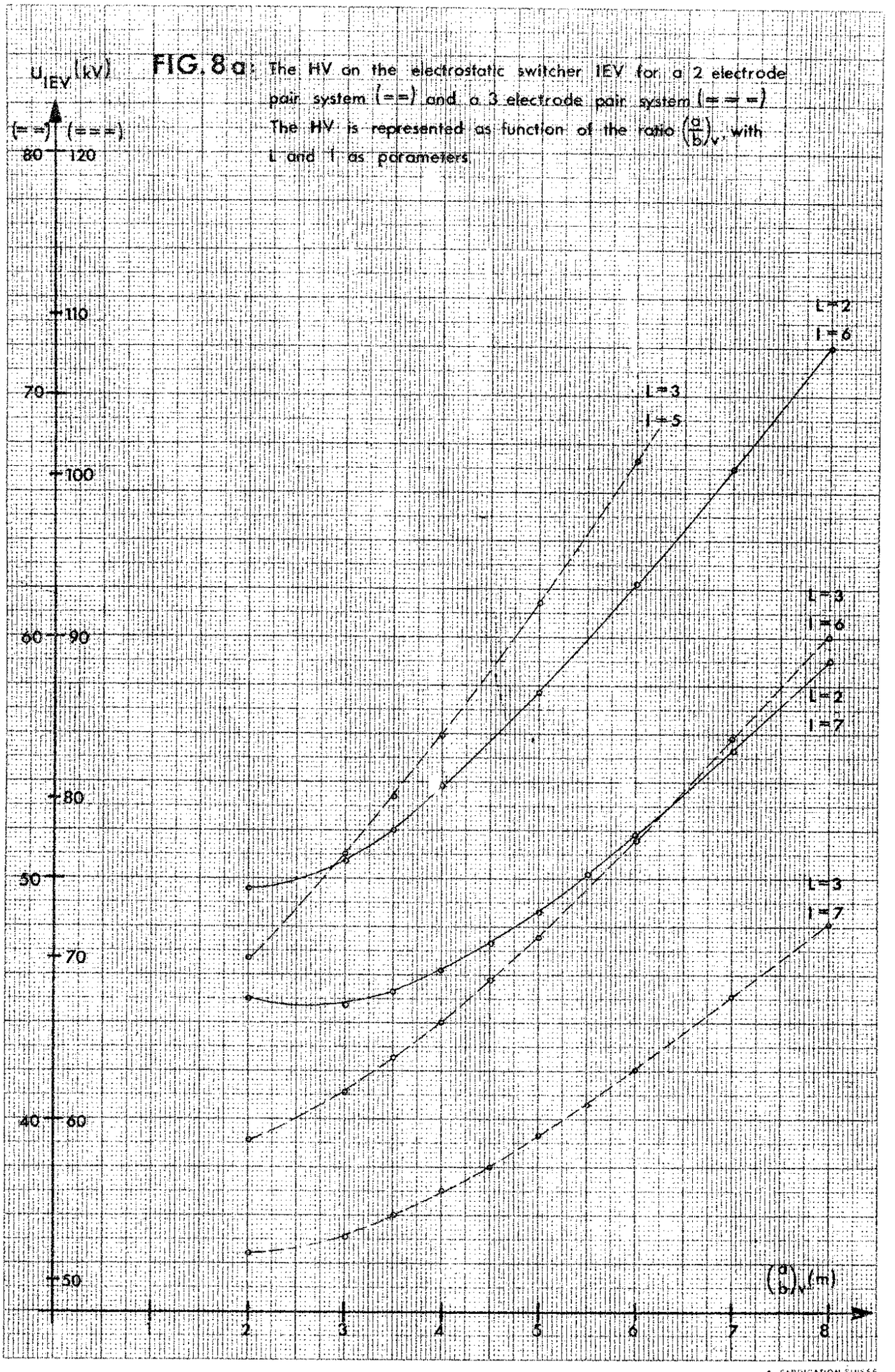

FIG. 8a: The HV on the electrostatic switcher IEV for a 2 electrode pair system (= =) and a 3 electrode pair system (= = =) The HV is represented as function of the ratio $\left(\frac{a}{b}\right)_V$, with L and l as parameters.

FABRICATION SUISSE

9.5.68 fadam

FIG. 9 : Minima of $f\left(\frac{a}{b}, x, L, l\right)$ as function of l and $\frac{a}{b}$. The position of waist corresponding to f min is indicated. L is taken as parameter.

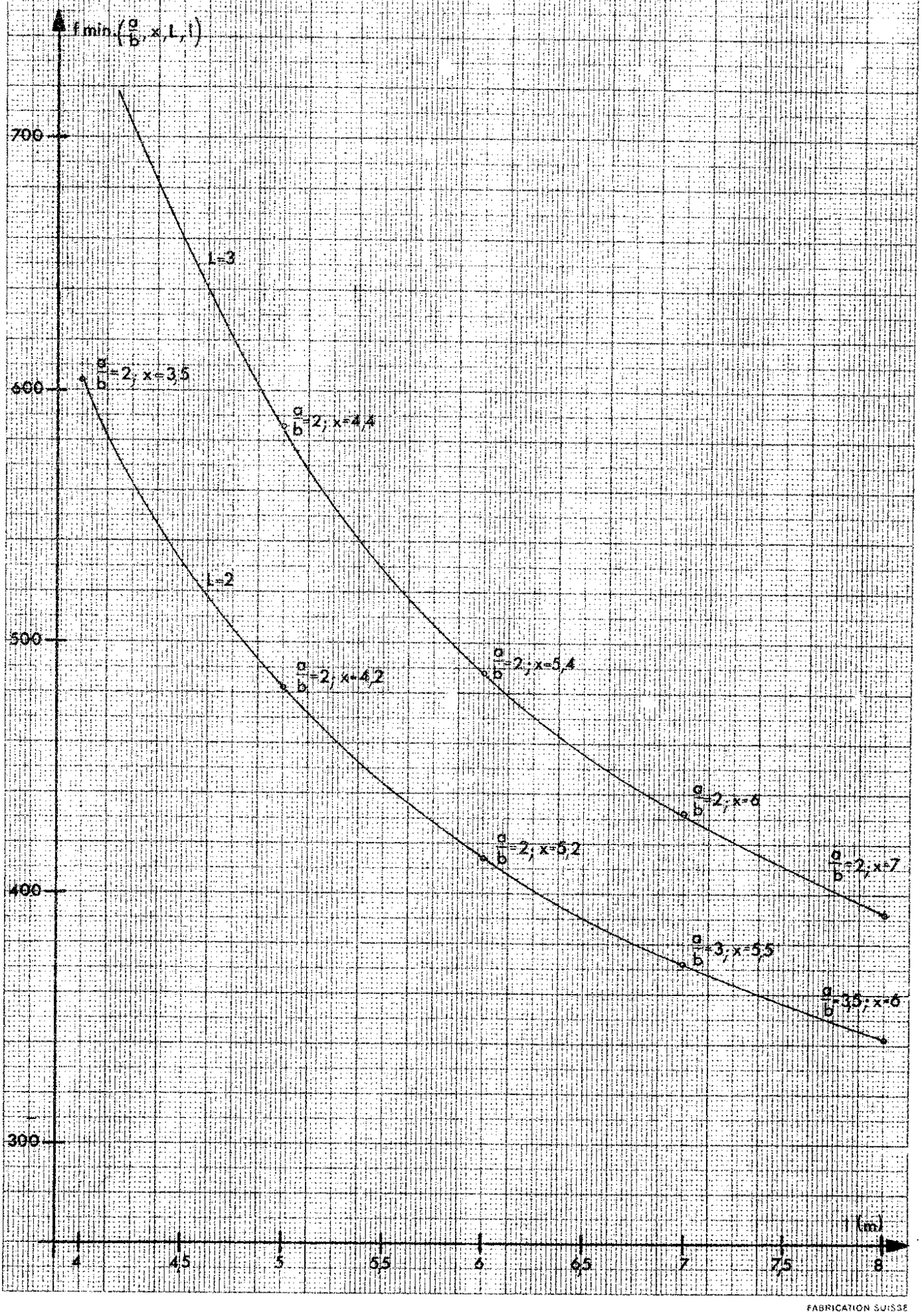

FIG. 10 : Relation between l_1 and l_2 for various ratios $\left(\frac{a}{b}\right)_v$ at waist.

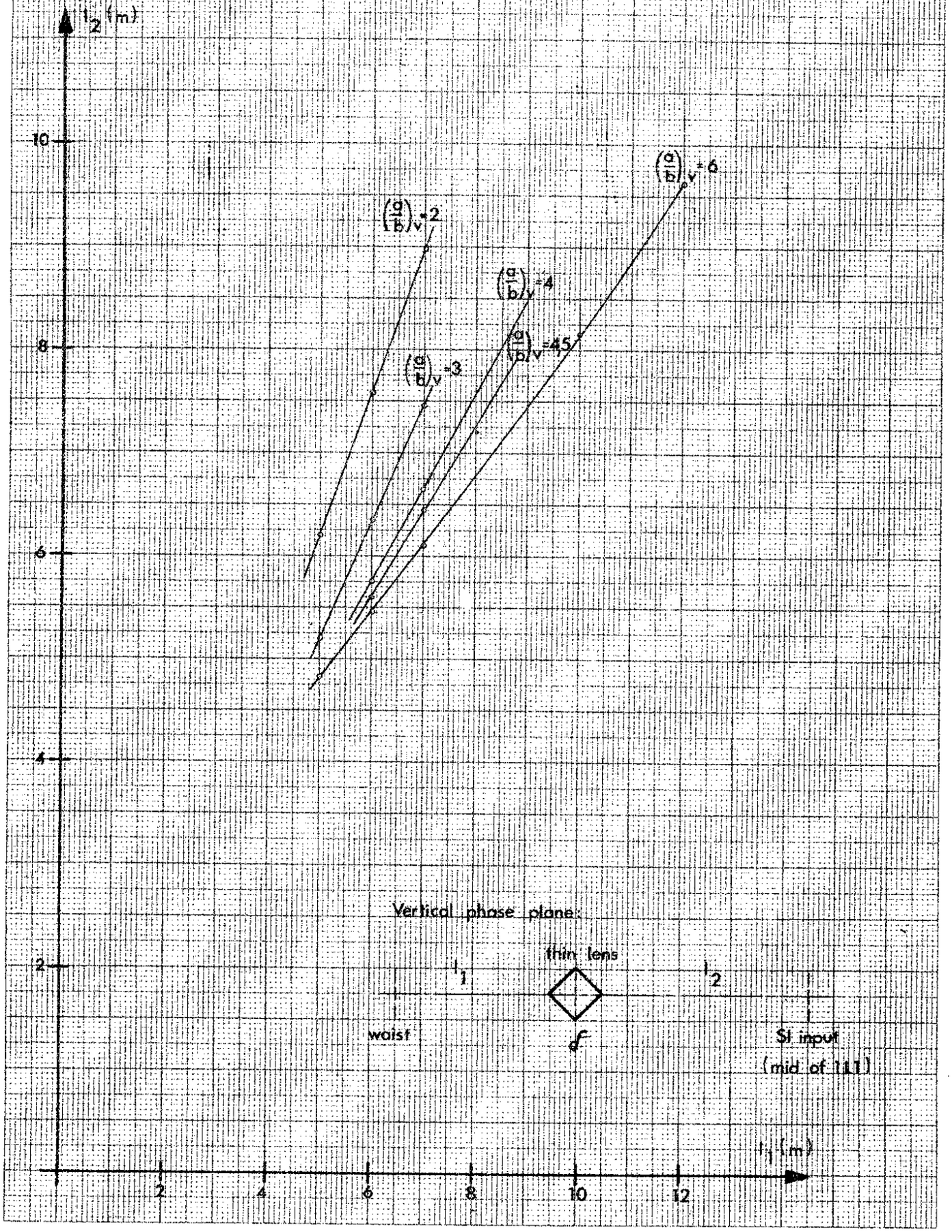

FABRICATION SUISSE

3.5.68

FIG. 11 a : Position of principal planes of a doublet

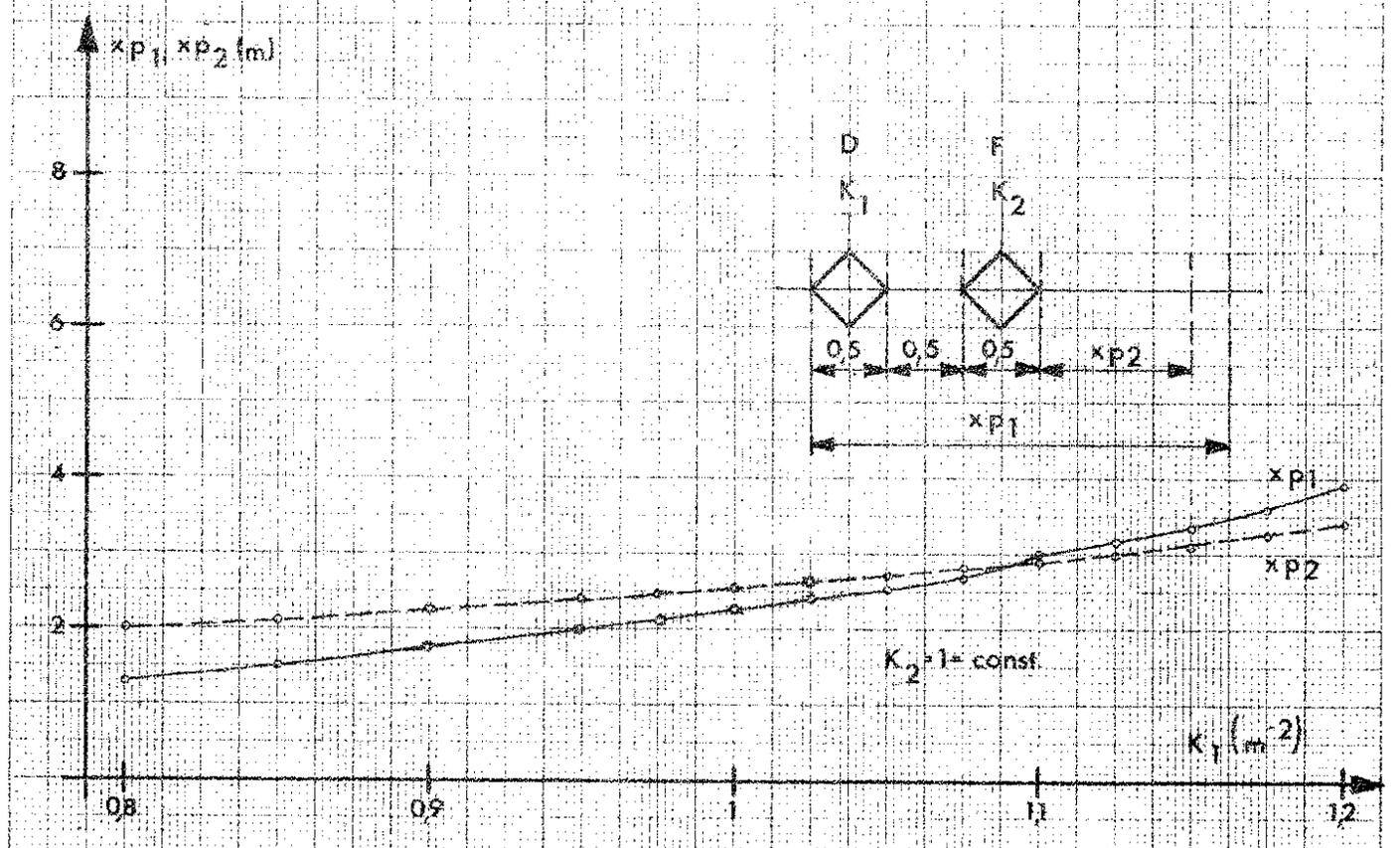

FIG. 11 b

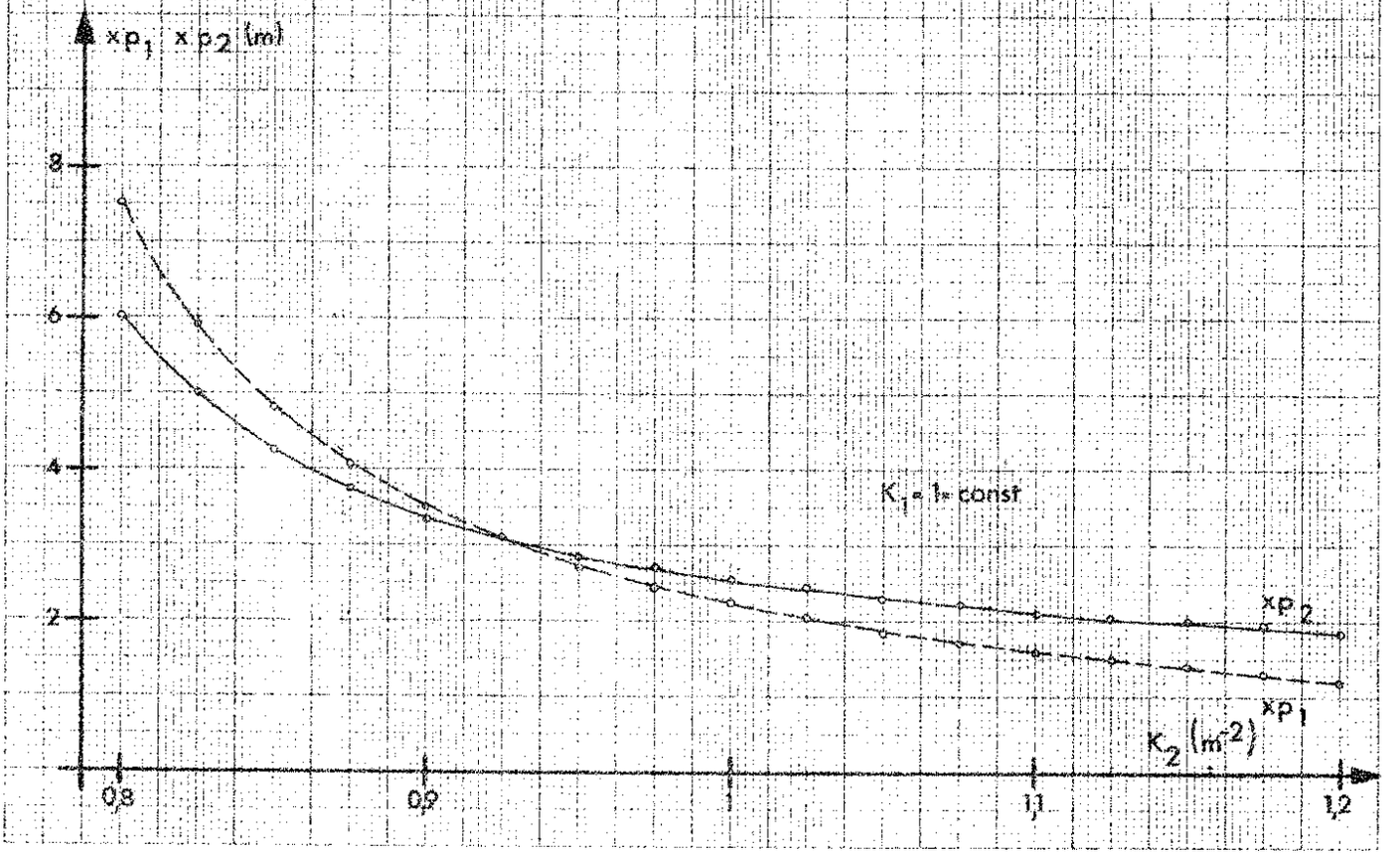

MPS 4158 105-1994-4

3.5.68 Landau

FIG. 11 c : Position of principal planes of a doublet

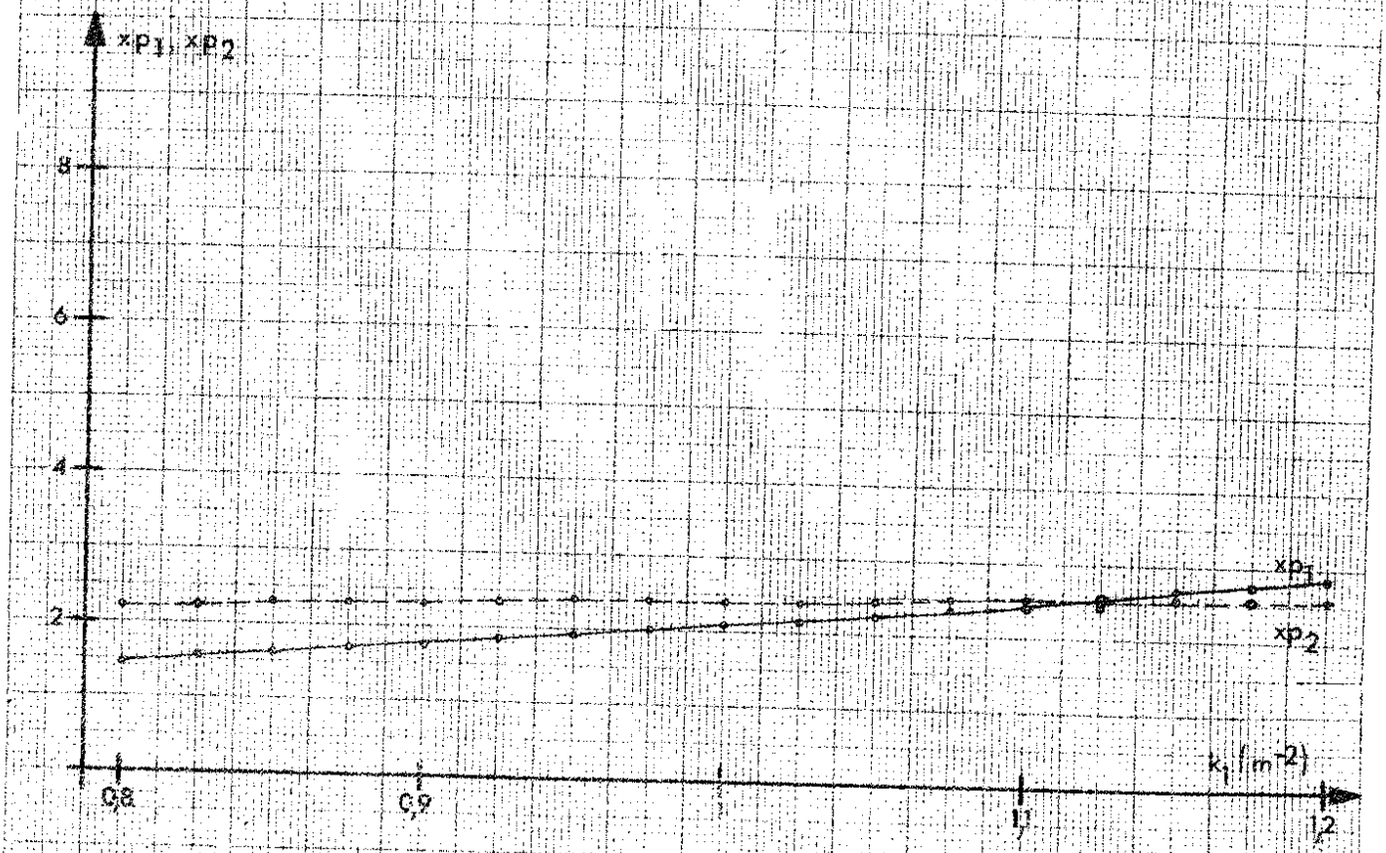

FIG. 11 d

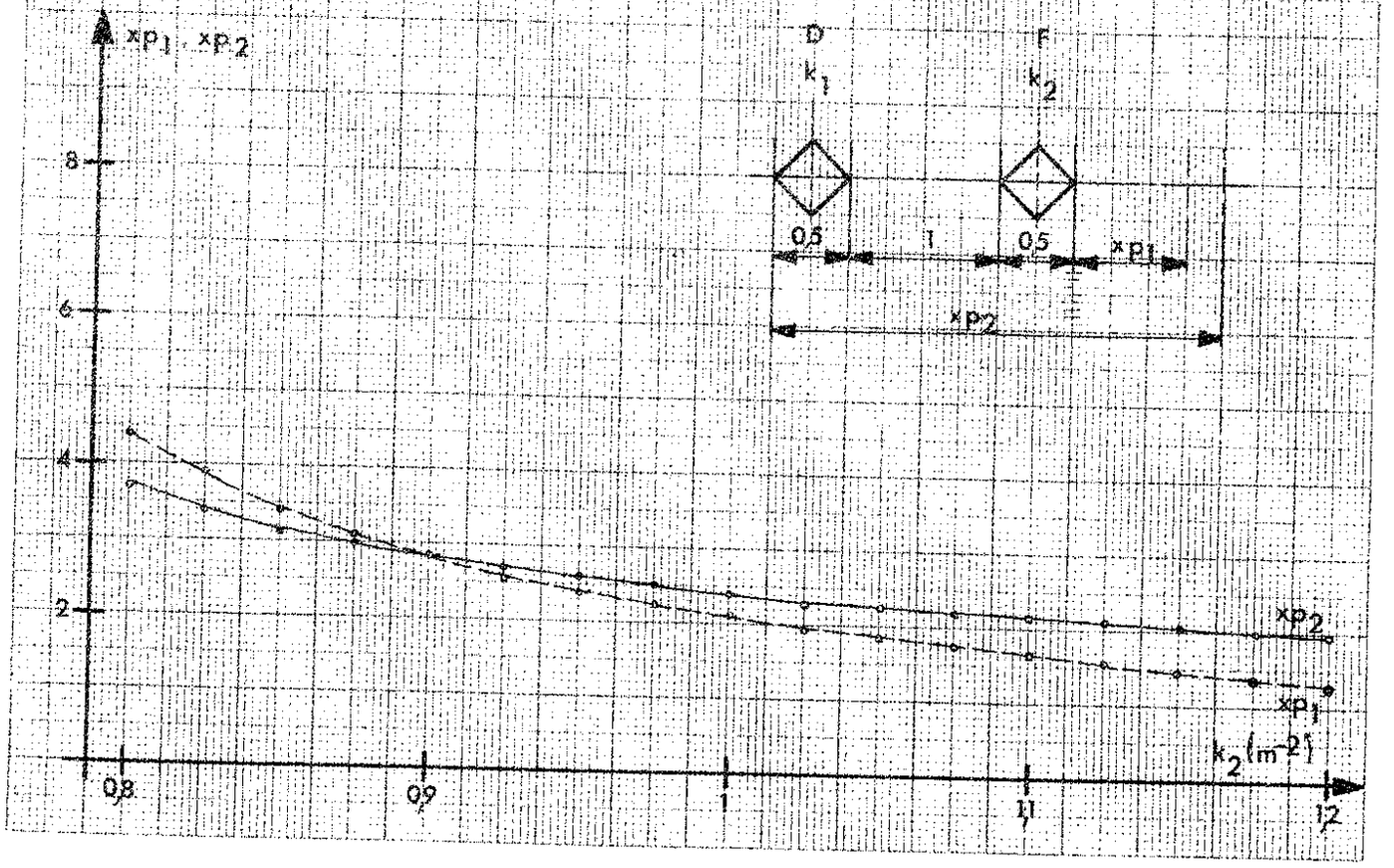

FABRICATION SUISSE

P.S. 68

FIG. 12: Horizontal phase plane beam radius at 3.15 m in front of SI input (mid of 1.L1). The ratio $\left(\frac{\alpha}{b}\right)_H$ is chosen corresponding to the no. of injected turns.

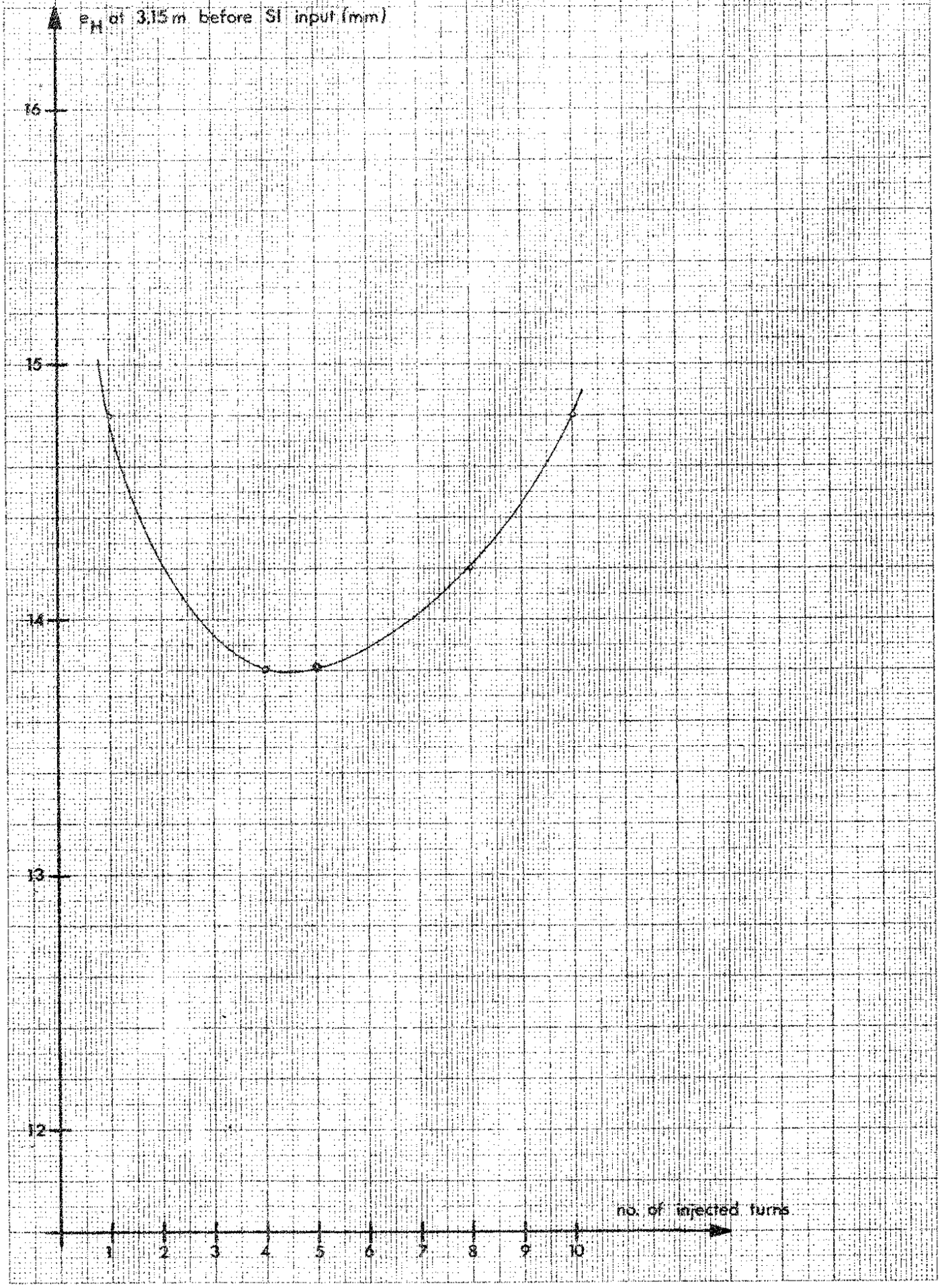

3.5.68

FIG. 13: Energy spread measurements

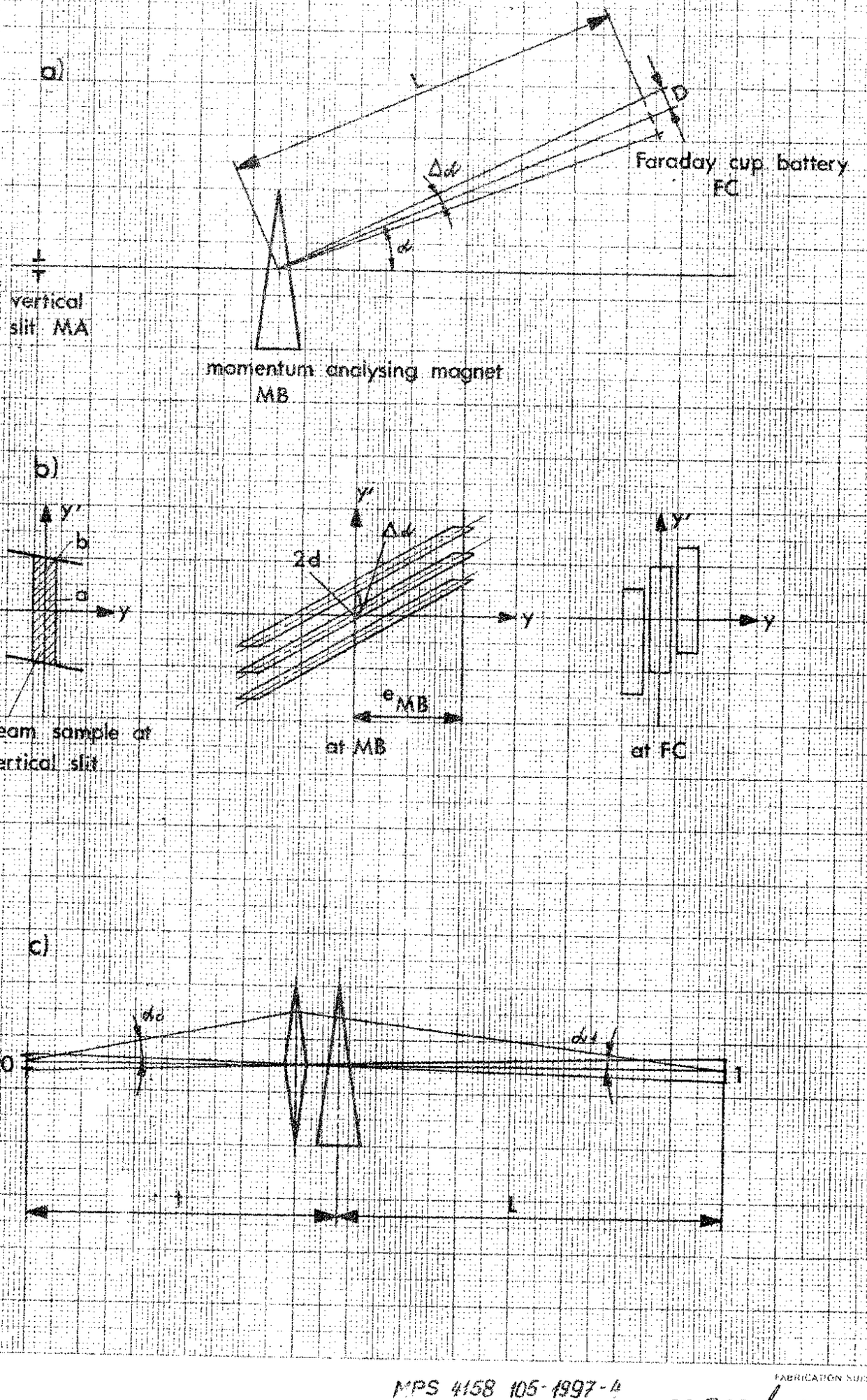

FIG. 14 a: Measuring line — principle

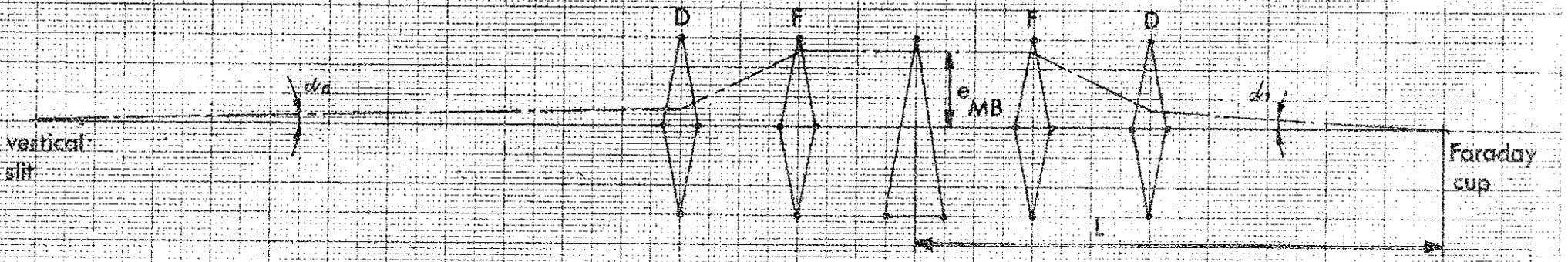

FIG. 14 b: Layout of the measuring line